

## Durham Research Online

---

### Deposited in DRO:

10 August 2017

### Version of attached file:

Accepted Version

### Peer-review status of attached file:

Peer-reviewed

### Citation for published item:

Wang, Shuijiong and Teng, Fang-Zhen and Li, Shu-Guang and Zhang, Li-Fei and Du, Jin-Xue and He, Yong-Sheng and Niu, Yaoling (2017) 'Tracing subduction zone fluid-rock interactions using trace element and Mg-Sr-Nd isotopes.', *Lithos.*, 290-291 . pp. 94-103.

### Further information on publisher's website:

<https://doi.org/10.1016/j.lithos.2017.08.004>

### Publisher's copyright statement:

© 2017 This manuscript version is made available under the CC-BY-NC-ND 4.0 license  
<http://creativecommons.org/licenses/by-nc-nd/4.0/>

### Additional information:

---

## Use policy

The full-text may be used and/or reproduced, and given to third parties in any format or medium, without prior permission or charge, for personal research or study, educational, or not-for-profit purposes provided that:

- a full bibliographic reference is made to the original source
- a [link](#) is made to the metadata record in DRO
- the full-text is not changed in any way

The full-text must not be sold in any format or medium without the formal permission of the copyright holders.

Please consult the [full DRO policy](#) for further details.

Manuscript Number: LITHOS6284R2

Title: Tracing subduction zone fluid-rock interactions using trace element and Mg-Sr-Nd isotopes

Article Type: Regular Article

Keywords: Mg isotopes; subduction channel; fluid-rock interaction; eclogite; Tianshan

Corresponding Author: Dr. Shuijiong Wang, Ph.D

Corresponding Author's Institution: China University of Geosciences

First Author: Shuijiong Wang, Ph.D

Order of Authors: Shuijiong Wang, Ph.D; Fang-Zhen Teng; Shu-Guang Li; Li-Fei Zhang; Jin-Xue Du; Yong-Sheng He; Yaoling Niu

**Abstract:** Slab-derived fluids play a key role in mass transfer and elemental/isotopic exchanges in subduction zones. The exhumation of deeply subducted crust is achieved via a subduction channel where fluids from various sources are abundant, and thus the chemical/isotopic compositions of these rocks could have been modified by subduction-zone fluid-rock interactions. Here, we investigate the Mg isotopic systematics of eclogites from southwestern Tianshan, in conjunction with major/trace element and Sr-Nd isotopes, to characterize the source and nature of fluids and to decipher how fluid-rock interactions in subduction channel might influence the Mg isotopic systematics of exhumed eclogites. The eclogites have high LILEs (especially Ba) and Pb, high initial  $^{87}\text{Sr}/^{86}\text{Sr}$  (up to 0.7117; higher than that of coeval seawater), and varying Ni and Co (mostly lower than those of oceanic basalts), suggesting that these eclogites have interacted with metamorphic fluids mainly released from subducted sediments, with minor contributions from altered oceanic crust or altered abyssal peridotites. The positive correlation between  $^{87}\text{Sr}/^{86}\text{Sr}$  and  $\text{Pb}^*$  (an index of Pb enrichment;  $\text{Pb}^* = 2 \times \text{PbN}/[\text{CeN} + \text{PrN}]$ ), and the decoupling relationships and bidirectional patterns in  $^{87}\text{Sr}/^{86}\text{Sr}$ -Rb/Sr,  $\text{Pb}^*$ -Rb/Sr and  $\text{Pb}^*$ -Ba/Pb spaces imply the presence of two compositionally different components for the fluids: one enriched in LILEs, and the other enriched in Pb and  $^{87}\text{Sr}/^{86}\text{Sr}$ . The systematically heavier Mg isotopic compositions ( $\delta^{26}\text{Mg} = -0.37$  to  $+0.26$ ) relative to oceanic basalts ( $-0.25 \pm 0.07$ ) and the roughly negative correlation of  $\delta^{26}\text{Mg}$  with MgO for the southwestern Tianshan eclogites, cannot be explained by inheritance of Mg isotopic signatures from ancient seafloor alteration or prograde metamorphism. Instead, the signatures are most likely produced by fluid-rock interactions during the exhumation of eclogites. The high Rb/Sr and Ba/Pb but low  $\text{Pb}^*$  eclogites generally have high bulk-rock  $\delta^{26}\text{Mg}$  values, whereas high  $\text{Pb}^*$  and  $^{87}\text{Sr}/^{86}\text{Sr}$  eclogites have mantle-like  $\delta^{26}\text{Mg}$  values, suggesting diverse influences of the two fluid components on the Mg isotopic systematics of these eclogites. The LILE-rich fluid component, possibly derived from mica-group minerals, contains a considerable amount of heavy Mg that has shifted  $\delta^{26}\text{Mg}$  of the eclogites towards higher values. By contrast, the  $^{87}\text{Sr}/^{86}\text{Sr}$ - and Pb-rich fluid component, most likely released from epidote-group minerals in

metasediments, has little Mg so as not to modify the Mg isotopic composition of the eclogites. In addition, the influence of talc-derived fluid might be evident in a very few eclogites that have low Rb/Sr and Ba/Pb but slightly heavier Mg isotopic compositions. These findings represent an important step toward a broad understanding of the Mg isotope geochemistry in subduction zones, and contributing to understanding why island arc basalts have averagely heavier Mg isotopic compositions than the normal mantle.

## **Abstract**

Slab-derived fluids play a key role in mass transfer and elemental/isotopic exchanges in subduction zones. The exhumation of deeply subducted crust is achieved via a subduction channel where fluids from various sources are abundant, and thus the chemical/isotopic compositions of these rocks could have been modified by subduction-zone fluid-rock interactions. Here, we investigate the Mg isotopic systematics of eclogites from southwestern Tianshan, in conjunction with major/trace element and Sr-Nd isotopes, to characterize the source and nature of fluids and to decipher how fluid-rock interactions in subduction channel might influence the Mg isotopic systematics of exhumed eclogites. The eclogites have high LILEs (especially Ba) and Pb, high initial  $^{87}\text{Sr}/^{86}\text{Sr}$  (up to 0.7117; higher than that of coeval seawater), and varying Ni and Co (mostly lower than those of oceanic basalts), suggesting that these eclogites have interacted with metamorphic fluids mainly released from subducted sediments, with minor contributions from altered oceanic crust or altered abyssal peridotites. The positive correlation between  $^{87}\text{Sr}/^{86}\text{Sr}$  and  $\text{Pb}^*$  (an index of Pb enrichment;  $\text{Pb}^* = 2 \times \text{Pb}_\text{N}/[\text{Ce}_\text{N} + \text{Pr}_\text{N}]$ ), and the decoupling relationships and bidirectional patterns in  $^{87}\text{Sr}/^{86}\text{Sr}$ -Rb/Sr,  $\text{Pb}^*$ -Rb/Sr and  $\text{Pb}^*$ -Ba/Pb spaces imply the presence of two compositionally different components for the fluids: one enriched in LILEs, and the other enriched in Pb and  $^{87}\text{Sr}/^{86}\text{Sr}$ . The systematically heavier Mg isotopic compositions ( $\delta^{26}\text{Mg} = -0.37$  to  $+0.26$ ) relative to oceanic basalts ( $-0.25 \pm 0.07$ ) and the roughly negative correlation of  $\delta^{26}\text{Mg}$  with MgO for the southwestern Tianshan eclogites, cannot be explained by inheritance of Mg isotopic signatures from

ancient seafloor alteration or prograde metamorphism. Instead, the signatures are most likely produced by fluid-rock interactions during the exhumation of eclogites. The high Rb/Sr and Ba/Pb but low Pb\* eclogites generally have high bulk-rock  $\delta^{26}\text{Mg}$  values, whereas high Pb\* and  $^{87}\text{Sr}/^{86}\text{Sr}$  eclogites have mantle-like  $\delta^{26}\text{Mg}$  values, suggesting diverse influences of the two fluid components on the Mg isotopic systematics of these eclogites. The LILE-rich fluid component, possibly derived from mica-group minerals, contains a considerable amount of heavy Mg that has shifted  $\delta^{26}\text{Mg}$  of the eclogites towards higher values. By contrast, the  $^{87}\text{Sr}/^{86}\text{Sr}$ - and Pb-rich fluid component, most likely released from epidote-group minerals in metasediments, has little Mg so as not to modify the Mg isotopic composition of the eclogites. In addition, the influence of talc-derived fluid might be evident in a very few eclogites that have low Rb/Sr and Ba/Pb but slightly heavier Mg isotopic compositions. These findings represent an important step toward a broad understanding of the Mg isotope geochemistry in subduction zones, and contributing to understanding why island arc basalts have averagely heavier Mg isotopic compositions than the normal mantle.

Highlights:

1. Tianshan eclogites were interacted with two fluid components during exhumation.
2. The high-LILEs component is likely released from mica-group minerals.
3. The high-LILEs component contains a significant amount of isotopically heavy Mg.
4. The high-Pb component is possibly dehydrated from epidote-group minerals.
5. The high-Pb component contains too little Mg so as not to influence the eclogites.

# Tracing subduction zone fluid-rock interactions using trace element and Mg-Sr-Nd isotopes

Shui-Jiong Wang<sup>1,2\*</sup>, Fang-Zhen Teng<sup>2\*</sup>, Shu-Guang Li<sup>1</sup>, Li-Fei Zhang<sup>3</sup>, Jin-Xue Du<sup>1,3</sup>, Yong-Sheng He<sup>1</sup>, Yaoling Niu<sup>4,5</sup>

<sup>1</sup> State Key Laboratory of Geological Processes and Mineral Resources, China University of Geosciences, Beijing 100083, China

<sup>2</sup> Isotope Laboratory, Department of Earth and Space Sciences, University of Washington, Seattle, WA 98195-1310, USA

<sup>3</sup> School of Earth Space Sciences, Peking University, Beijing, China

<sup>4</sup> Institute of Oceanology, Chinese Academy of Sciences, Qingdao 266071, China

<sup>5</sup> Department of Earth Sciences, Durham University, Durham DH1 3LE, UK

Abstract: 492 words

Text: 5139 words

Figure: 6

Table: 2

Revised version submitted to *Lithos* (July 29, 2017)

\*Present address: Department of Earth and Atmospheric Sciences, Indiana University, Bloomington, IN 47405 USA.

Corresponding authors: [sxw057@gmail.com](mailto:sxw057@gmail.com)(S.-J. Wang); [fteng@u.washington.edu](mailto:fteng@u.washington.edu) (F.-Z. Teng)

## Abstract

Slab-derived fluids play a key role in mass transfer and elemental/isotopic exchanges in subduction zones. The exhumation of deeply subducted crust is achieved via a subduction channel where fluids from various sources are abundant, and thus the chemical/isotopic compositions of these rocks could have been modified by subduction-zone fluid-rock interactions. Here, we investigate the Mg isotopic systematics of eclogites from southwestern Tianshan, in conjunction with major/trace element and Sr-Nd isotopes, to characterize the source and nature of fluids and to decipher how fluid-rock interactions in subduction channel might influence the Mg isotopic systematics of exhumed eclogites. The eclogites have high LILEs (especially Ba) and Pb, high initial  $^{87}\text{Sr}/^{86}\text{Sr}$  (up to 0.7117; higher than that of coeval seawater), and varying Ni and Co (mostly lower than those of oceanic basalts), suggesting that these eclogites have interacted with metamorphic fluids mainly released from subducted sediments, with minor contributions from altered oceanic crust or altered abyssal peridotites. The positive correlation between  $^{87}\text{Sr}/^{86}\text{Sr}$  and  $\text{Pb}^*$  (an index of Pb enrichment;  $\text{Pb}^* = 2 \times \text{Pb}_\text{N}/[\text{Ce}_\text{N} + \text{Pr}_\text{N}]$ ), and the decoupling relationships and bidirectional patterns in  $^{87}\text{Sr}/^{86}\text{Sr}$ -Rb/Sr,  $\text{Pb}^*$ -Rb/Sr and  $\text{Pb}^*$ -Ba/Pb spaces imply the presence of two compositionally different components for the fluids: one enriched in LILEs, and the other enriched in Pb and  $^{87}\text{Sr}/^{86}\text{Sr}$ . The systematically heavier Mg isotopic compositions ( $\delta^{26}\text{Mg} = -0.37$  to  $+0.26$ ) relative to oceanic basalts ( $-0.25 \pm 0.07$ ) and the roughly negative correlation of  $\delta^{26}\text{Mg}$  with MgO for the southwestern Tianshan eclogites, cannot be explained by inheritance of Mg isotopic signatures from ancient seafloor alteration or prograde metamorphism. Instead, the signatures are most likely produced by fluid-rock interactions during the exhumation of



eclogites. The high Rb/Sr and Ba/Pb but low Pb\* eclogites generally have high bulk-rock  $\delta^{26}\text{Mg}$  values, whereas high Pb\* and  $^{87}\text{Sr}/^{86}\text{Sr}$  eclogites have mantle-like  $\delta^{26}\text{Mg}$  values, suggesting that the two fluid components have diverse influences on the Mg isotopic systematics of these eclogites. The LILE-rich fluid component, possibly derived from mica-group minerals, contains a considerable amount of isotopically heavy Mg that has shifted the  $\delta^{26}\text{Mg}$  of the eclogites towards higher values. By contrast, the  $^{87}\text{Sr}/^{86}\text{Sr}$ - and Pb-rich fluid component, most likely released from epidote-group minerals in metasediments, has little Mg so as not to modify the Mg isotopic composition of the eclogites. In addition, the influence of talc-derived fluid might be evident in a very few eclogites that have low Rb/Sr and Ba/Pb but slightly heavier Mg isotopic compositions. These findings represent an important step toward a broad understanding of the Mg isotope geochemistry in subduction zones, and contributing to understanding why island arc basalts have averagely heavier Mg isotopic compositions than the normal mantle.

**Keywords:** Mg isotopes, subduction channel, fluid-rock interaction, eclogite, Tianshan

## 1. Introduction

Subduction channel is a highly reactive interface between subducting oceanic lithosphere and mantle wedge, in which mass transfer as well as elemental and isotopic exchanges actively occur (*e.g.*, Bebout and Penniston-Dorland, 2016). In this region, fluids released from various subducting slab lithologies (*e.g.*, sediments, altered oceanic crust, and altered abyssal peridotites) can be mixed and penetrate into exhuming rocks, inducing extensive fluid-rock interactions (Zack and John, 2007; John et al., 2008; van der Straaten et al., 2008, 2012). The fluids, when emanating from the interface into the mantle wedge, can further impart their chemical/isotopic signatures to the juxtaposed mantle rocks and associated arc volcanism.

Trace elements in conjunction with Sr-Nd-O isotopic systematics have been widely used to identify and understand fluid-rock interactions in subduction channels (Glodny et al., 2003; John et al., 2004, 2012; King et al., 2006; Halama et al., 2011). The magnesium (Mg) isotopic systematics might be a useful tracer of subduction-zone fluid-rock interactions, potentially providing insights into the source and nature of fluids. Magnesium is fluid-mobile at low temperatures, which leads to large Mg isotope fractionations as much as 7 ‰ during Earth's surface processes (Teng, 2017 and references therein). Recent studies also documented high mobility of Mg during subduction-zone metamorphism (van der Straaten et al., 2008; Horodyskyj et al., 2009; Pogge von Strandmann et al., 2015; Chen et al., 2016). Chen et al. (2016) found high  $\delta^{26}\text{Mg}$  values (up to +0.72) for white schists from Western Alps, and linked them to infiltration of Mg-rich fluids derived from dehydration of

serpentinites. Recent studies also documented generally heavier Mg isotopic compositions in arc volcanic rocks relative to normal peridotitic sources ( $\delta^{26}\text{Mg} = -0.25 \pm 0.07$ ), which were explained as the addition of heavy Mg isotopes from subducting slabs to the mantle wedge (Teng et al., 2016; Li et al., 2017). A general conclusion derived from these studies is that the subduction-zone fluids might be isotopically heavy in terms of Mg isotopes. Nevertheless, the interpretation of any Mg isotopic variations in subduction-related rocks requires the knowledge of how Mg isotopes behave in subduction channels, and how fluid-rock interactions could affect the Mg isotopic systematics of a rock.

Orogenic eclogites of seafloor protolith may be the best choice to study subduction channel processes. Oceanic crust undergoes seawater alteration prior to subduction and is, therefore, more hydrated relative to the continental crust (Miller et al., 1988). It experiences extensive dehydration together with the sediment veneer during subduction (Gerya et al., 2002). In addition, the exhumation of oceanic crust via the subduction channel proceeds at relatively slower rate (mm/yr; Agard et al., 2009). All of these allow eclogites of seafloor protolith to preserve a record of extensive fluid-rock interactions during exhumation. An increasing number of studies have shown that fluid-rock interactions can readily modify the chemical and isotopic compositions of exhumed eclogites (*e.g.*, Bebout, 2007; Xiao et al., 2012; Klemd, 2013), although how the chemical/isotopic composition shift depends on the nature and abundance of fluids with which the eclogites have interacted.

In this study, we investigate a suite of well-characterized eclogites/blueschists and mica schists from southwestern Tianshan, China. We present the first Mg isotopic data for the

orogenic eclogites of seafloor protolith, and in combination with Sr-Nd isotopic and trace elemental data, we explore the influence of subduction-zone fluid-rock interactions on the Mg isotopic systematics of eclogites. Our results show that these eclogites are variably enriched in heavy Mg isotopes, which may result from interactions of the eclogites with both high-MgO and low-MgO fluids released from different hydrous minerals in the subduction channel.

## **2. Geological settings and samples**

The high-pressure to ultrahigh-pressure (HP-UHP) metamorphic belt of Chinese southwestern Tianshan, located along the suture between the Yili and the Tarim blocks, was formed during the northward subduction of the Palaeo-South Tianshan oceanic crust beneath the Yili block (Windley et al., 1990; Gao et al., 1999; Zhang et al., 2002, 2008). The eclogites and retrograded blueschists in southwestern Tianshan occur as interlayers or lenticular bodies in mica schists, representing the relic oceanic crust that experienced subduction and exhumation in response to later continental collision. The protoliths of eclogites and associated blueschists range from MORBs to OIBs as indicated by the geochemical data and their preserved pillow structures in the field (Zhang et al., 2002, 2008; Gao and Klemd, 2003; Ai et al., 2006). The eclogites and their host rocks have experienced peak coesite-bearing eclogite-facies metamorphism at 324 ~ 312 Ma (Zhang et al., 2005; Su et al., 2010; Klemd et al., 2011; Li et al., 2011a; Yang et al., 2013), followed by a slow exhumation rate to amphibolite-facies between 320 Ma and 240 Ma (*e.g.*, Zhang et al., 2013). The peak and retrograde metamorphic temperatures estimated for the southwestern Tianshan eclogites vary

from 450 to 630 °C (*e.g.*, Du et al., 2014a, b). The retrograde metamorphic temperatures are slightly higher than the peak-eclogite facies temperatures as a result of thermal relaxation during the exhumation (*e.g.*, Zhang et al., 2013). The presence of abundant millimeter to decimeter-wide and centimeter to meter-long veins in southwestern Tianshan blueschists and eclogites indicates extensive fluid-rock interactions and fluid-mediated mass transport during crustal subduction and exhumation (Gao and Klemd, 2001; Gao et al., 2007; John et al., 2008; 2012; Beinlich et al., 2010; Lü et al., 2012).

The petrology and metamorphic evolution of the studied eclogites and mica schists have been well characterized (Zhang et al., 2003; Ai et al., 2006; Lü et al., 2009; Du et al., 2011, 2014b; Xiao et al., 2012). The eclogites consist mainly of garnet, omphacite, glaucophane, paragonite, epidote, calcite, dolomite and quartz/coesite; the mica schists are mainly composed of garnet, glaucophane, phengite, epidote, paragonite, plagioclase and quartz/coesite. A detail description of the studied eclogites and mica schists including the sample localities has been given in Supplementary Table S1.

### **3. Analytical methods**

#### **3.1 Major and trace elements**

Major elements were analyzed at the Hebei Institute of Regional Geology and Mineral Resources, China, by wavelength dispersive X-Ray fluorescence spectrometry (Gao et al., 1995). Analytical uncertainties are generally better than 1%. The H<sub>2</sub>O<sup>+</sup> and CO<sub>2</sub> were determined by gravimetric methods and potentiometry, respectively. Trace elements were analyzed using an Elan 6100 DRC ICP-MS at the CAS key laboratory of crust-material and

environments, University of Science and Technology of China, Hefei. Samples were analyzed with aliquots of USGS whole-rock standards BHVO-2, BIR-1, AGV-2 and GSP-2, which were treated as unknown. Results for the USGS standards together with the reference values are reported in Supplementary Table S2. Analytical uncertainties are better than 5% for most of the elements.

### 3.2 Strontium and Nd isotopic analysis

The Sr and Nd were separated from the matrix with cation exchange chromatography with Bio-Rad AG50W-X12 resin using the method described by Chu et al. (2009). The Sr and Nd isotopes were performed using an Isoprobe-T thermal ionization mass spectrometer (TIMS) at the State Key Laboratory of Lithospheric Evolution, Institute of Geology and Geophysics, Chinese Academy of Sciences. Measured  $^{87}\text{Sr}/^{86}\text{Sr}$  and  $^{143}\text{Nd}/^{144}\text{Nd}$  ratios were corrected for mass-fractionation using  $^{86}\text{Sr}/^{88}\text{Sr} = 0.1194$  and  $^{146}\text{Nd}/^{144}\text{Nd} = 0.7219$ , respectively. During the course of this study, standards of NBS987-Sr and jNdi-Nd give a value of  $^{87}\text{Sr}/^{86}\text{Sr} = 0.710245 \pm 20$  and  $^{143}\text{Nd}/^{144}\text{Nd} = 0.512117 \pm 10$ , respectively.

### 3.3 Magnesium isotopic analysis

Magnesium isotopic ratios were analyzed for bulk rock powders and mineral separates at the University of Washington, Seattle. The separation of Mg was achieved by cation exchange chromatography using Bio-Rad AG50W-X8 resin in 1N HNO<sub>3</sub> media (Teng et al., 2007, 2010a; 2015; Yang et al., 2009; Li et al., 2010). Two standards, Kilbourne Hole (KH) olivine and seawater, were processed together with samples for each batch of column chemistry. The Mg isotopic ratios were determined using the standard-sample bracketing

protocol on a *Nu* plasma MC-ICPMS (Teng and Yang, 2014). The blank Mg signal for  $^{24}\text{Mg}$  was  $< 10^{-4}$  V, which is negligible relative to the sample signals of 3-5 V. The KH olivine and seawater yielded average  $\delta^{26}\text{Mg}$  of  $-0.25 \pm 0.05$  and  $-0.82 \pm 0.06$ , respectively, consistent with previous reported values (Foster et al., 2010; Li et al., 2010; Teng et al., 2010; Ling et al., 2011; Wang et al., 2016)

## 4. Results

Major and trace elemental compositions of the eclogites and mica schists are summarized in Supplementary Table S3. The eclogites have  $\text{SiO}_2$  ranging from 39.82 to 52.47 wt.% and MgO ranging from 3.19 to 9.68 wt.% (Supplementary Table S3), and plot in subalkalic basalt field in Zr/Ti versus Nb/Y diagram (Supplementary Fig. S1; Pearce, 1996). The high contents of  $\text{H}_2\text{O}^+$  (0.58 to 3.38 wt.%) and  $\text{CO}_2$  (0.08 to 8.96 wt.%) are consistent with the presence of water- and/or carbon oxide-bearing minerals such as zoisite/clinozoisite and calcite/dolomite. The eclogites have variably high LILEs (*e.g.*, Ba, Rb, Cs, and K) and Pb, but low Ni and Co concentrations (Supplementary Table S3). The mica schists are felsic with  $\text{SiO}_2$  ranging from 59.53 to 76.66 wt.% and MgO ranging from 1.81 to 3.60 wt.% (Supplementary Table S3). They are characterized by variable contents of LILEs, Sr and Pb, which may be controlled by different proportions of mica-group minerals (host of LILEs) and epidote-group minerals (major host of Sr and Pb) in southwestern Tianshan metasediments (*e.g.*, Xiao et al., 2012).

The Sr and Nd isotopic compositions of the eclogites are reported in Table 1. The eclogites have positive age-corrected  $\epsilon\text{Nd}_{320\text{Ma}}$  value ranging from +2.8 to +10.1 (with one

exception of -2.4; Fig. 1). They have extremely high and variable initial Sr isotopic compositions ( $^{87}\text{Sr}/^{86}\text{Sr}_{320\text{Ma}}$ ) varying from 0.7058 to 0.7117 (Fig. 1), a range that is even higher than that of Ordovician to Carboniferous seawater ( $^{87}\text{Sr}/^{86}\text{Sr} = 0.7075 - 0.7090$ ; Veizer, 1989). As a result, the eclogites plot rightward far from the field defined by depleted MORB and OIB in  $\epsilon\text{Nd}(t) - ^{87}\text{Sr}/^{86}\text{Sr}(t)$  diagram (Fig. 1).

The  $\delta^{26}\text{Mg}$  values of southwestern Tianshan eclogites vary widely from  $-0.37 \pm 0.05$  to  $+0.26 \pm 0.04$  (Table 2), equal to or higher than unaltered oceanic basalts and eclogites of continental basalt protolith, both of which have homogeneous Mg isotopic compositions around the normal mantle value ( $-0.25 \pm 0.07$ ; Fig. 2). Garnets in southwestern Tianshan eclogites yield  $\delta^{26}\text{Mg}$  values varying from  $-1.75 \pm 0.07$  to  $-1.10 \pm 0.07$ , and omphacites have  $\delta^{26}\text{Mg}$  values ranging from  $-0.04 \pm 0.05$  to  $+0.46 \pm 0.07$  (Table 2), with corresponding inter-mineral Mg isotope fractionation ( $\Delta^{26}\text{Mg}_{\text{Cpx-Grt}} = \delta^{26}\text{Mg}_{\text{Cpx}} - \delta^{26}\text{Mg}_{\text{Grt}}$ ) in the range of 1.23 - 1.98. Temperatures estimated using garnet-clinopyroxene Mg isotope geothermometer range from 485°C to 675°C (Huang et al., 2013; Li et al., 2016b), which are in rough agreement with the peak and retrograde metamorphic temperatures for the Tianshan eclogites (e.g., Du et al., 2014a, b). Six mica schists from southwestern Tianshan have bulk  $\delta^{26}\text{Mg}$  values ranging from  $-0.11 \pm 0.05$  to  $+0.23 \pm 0.02$  (Table 2).

## 5. Discussion

The overprint of fluid-rock interactions on the southwestern Tianshan eclogites/blueschists has been confirmed by many petrological and geochemical studies (John et al., 2008; van der Straaten et al., 2008, 2012; Beinlich et al., 2010; Lü et al., 2012; Li et al.,



2016a; Zhang et al., 2016). Depending on the nature and abundance of fluids in a subduction channel, the initial composition of an eclogite can be altered to various degrees after fluid-rock interactions. In this section, we first focus on the trace element and Sr-Nd isotopes to characterize the source and nature of the fluids, and then decipher how fluid-rock interactions may have influenced the Mg isotopic systematics of the eclogites. Finally, we discuss the Mg isotope geochemistry of slab-derived fluids in the subduction channel and their influences on the sub-arc peridotites.

## 5.1 Geochemical evidence for fluid-rock interactions

Trace element and Sr-Nd isotope geochemistry suggest interactions of eclogites with metamorphic fluids. The fluids are mainly derived from subducted sediments, with limited contributions from serpentinites or altered oceanic crusts. Most eclogites are variably enriched in LILEs (*e.g.*, Ba, Cs, Rb, and K) and Pb (Fig. 3), which can be produced during either ancient seafloor alteration or subduction-zone fluid-rock interactions. Bebout (2007) documented that significant enrichments of Ba and Pb in metabasaltic rocks can be most directly associated with metasomatism because these two elements are only slightly enriched in altered oceanic basalts during seafloor alteration relative to other LILEs. The consistently high Ba/Rb, high Ba/K and low Ce/Pb of our eclogites are thus indicative of HP/UHP fluid-rock interactions rather than ancient seawater alteration (Fig. 3a, b, c). Furthermore, these eclogites have extremely high initial  $^{87}\text{Sr}/^{86}\text{Sr}$  ratio up to 0.7117 (Fig. 1), a signature that cannot be attributed to pre-subduction seawater alteration because the Ordovician-Carboniferous seawater has much lower  $^{87}\text{Sr}/^{86}\text{Sr}$  ratios of 0.7075 - 0.7090

(Veizer, 1989). The high  $^{87}\text{Sr}/^{86}\text{Sr}_{320\text{Ma}}$  ratios thus must have resulted from interactions of the eclogites with fluids during metasomatism, and the fluids might be derived from subducted sediments whose  $^{87}\text{Sr}/^{86}\text{Sr}$  ratios can be as high as 0.73 (Plank and Langmuir, 1998). In contrast to Sr isotopes, Nd isotopes appear to behave conservatively during the metasomatism (King et al., 2006). Due to the low mobility of REE during metamorphic dehydration under relatively low P-T conditions (Kessel et al., 2005), slab-derived fluids would contain too little Nd to affect the Nd isotopic systematics of eclogites (van der Straaten et al., 2012), such that the eclogites retain their depleted Nd isotopic signatures (Fig. 1). In accordance with the high  $^{87}\text{Sr}/^{86}\text{Sr}$  ratios, most eclogites contain very low concentrations of Co and Ni evolving from oceanic basalts towards the GLOSS (global subducting sediments; Fig. 3d), pointing towards again interactions of the eclogites with sediment-derived fluids. Some eclogites however have Ni and Co contents overlapping or slightly higher than oceanic basalts (Fig. 3d). This indicates the possible contributions of altered oceanic crust-derived or serpentinite-derived fluids (*e.g.*, van der Straaten et al., 2012), although subducted sediments must be the dominant source for fluids that have interacted with the eclogites.

The geochemical signatures of sediment-derived fluids might vary significantly in response to the mineralogical heterogeneity of subducting sediments. The eclogites display a series of geochemical features indicative of two compositionally different fluid components (Fig. 4). As shown in Rb/Sr vs. Pb\* (an index of enrichment of Pb;  $\text{Pb}^* = 2 \cdot \text{Pb}_\text{N}/[\text{Ce}_\text{N} + \text{Pr}_\text{N}]$ ) and Ba/Pb vs. Pb\* diagrams, the enrichment of Pb in eclogites is not always associated with the enrichment of LILEs (Fig. 4a and b). The observed decoupling patterns may indicate two major fluid components: one enriched in LILEs relative to Pb (*e.g.*, high Rb/Sr and Ba/Pb but

249 low Pb\*), and the other enriched in Pb relative to LILEs (*e.g.*, high Pb\* but low Rb/Sr or  
 250 Ba/Pb). The roughly positive correlation between Pb\* and  $^{87}\text{Sr}/^{86}\text{Sr}_{320\text{Ma}}$  (Fig. 4c), suggests  
 251 that the high-Pb component also contains a significant amount of radiogenic Sr that has  
 252 elevated the  $^{87}\text{Sr}/^{86}\text{Sr}$  value of eclogites. Some carbonated eclogites are extremely enriched in  
 253 elemental Sr but have relatively low  $^{87}\text{Sr}/^{86}\text{Sr}$  values of 0.7066 – 0.7078 (Supplementary Fig.  
 254 S2), suggesting that the surrounding marbles are not the source of high- $^{87}\text{Sr}/^{86}\text{Sr}$  fluid. Instead,  
 255 the high- $^{87}\text{Sr}/^{86}\text{Sr}$  fluid component must be sourced from other metasediments, such as mica  
 256 schists. The high-LILEs component, on the other hand, might contain too little Sr to modify  
 257 the Sr isotopic composition of eclogites, as reflected by the decoupling relationship between  
 258  $^{87}\text{Sr}/^{86}\text{Sr}_{320\text{Ma}}$  and Rb/Sr (Fig. 4d): the high-Rb/Sr eclogites display low  $^{87}\text{Sr}/^{86}\text{Sr}_{320\text{Ma}}$  values,  
 259 whereas the low-Rb/Sr samples are characterized by highly radiogenic Sr isotopic  
 260 compositions (Fig. 4d). All these observations support that the eclogites were infiltrated by  
 261 two fluid components. The distinct geochemical signatures of the two fluid components are  
 262 consistent with the fact that LILEs and Sr-Pb are hosted in different hydrous minerals in  
 263 subducted sediments: mica-group minerals are the dominant host for LILEs, whereas  
 264 epidote-group minerals (and to a less extent carbonate minerals and paragonite) are the major  
 265 host of Pb and Sr (*e.g.*, Busigny et al., 2003; Bebout et al., 2007, 2013; Xiao et al., 2012). As  
 266 a result, fluid dehydrated from mica-group minerals would have high Rb/Sr and Ba/Pb ratios,  
 267 whereas fluid released from epidote-group minerals in metasediments could be enriched in  
 268 Pb and Sr (as well as  $^{87}\text{Sr}/^{86}\text{Sr}$ ). It is possible that varying modal mineralogy in the subducted  
 269 sediments (*e.g.*, mica-group minerals are abundant in metapelites and epidote-group minerals  
 270 are abundant in greywackes) can result in decomposition of mica- and epidote-group

minerals in different proportions along the subduction P-T path and generate the two fluid components in the subduction channel. During crustal subduction, biotite is thought to be completely decomposed at  $P = 1.3\text{--}1.5$  GPa, at which the epidote-group minerals such as epidote and zoisite are still stable (Poli and Schmidt, 2002). Therefore, decomposition of biotite at the early stage during crustal subduction could release a significant amount of fluid that is enriched in LILEs. At a higher pressure above 2.5 GPa, epidote and zoisite might become unstable (Carswell, 1990; Poli and Schmidt, 2002). Metamorphic dehydration at this stage could thus release abundant Sr and Pb to the fluids. Such fluids, when released from subducting oceanic crust, would migrate upward along the subduction channel, infiltrate the exhuming eclogites and impart their distinct geochemical signatures to the eclogites via fluid-rock interactions.

## **5.2 Constraining the mechanisms of Mg isotopic variations in the eclogites**

The eclogites have varying Mg contents ( $\text{MgO} = 3.2$  to  $9.7$  wt.%) at a given  $\text{SiO}_2$  content, and more variable and systemically heavier Mg isotopic composition than fresh oceanic basalts (Fig. 5). The simplest explanation for the low MgO and high  $\delta^{26}\text{Mg}$  of eclogites is physical/mechanical mixing with a high- $\delta^{26}\text{Mg}$  sedimentary component at some point before or during the exhumation of the eclogites. However, this is very unlikely because binary mixing calculation, using the highest  $\delta^{26}\text{Mg}$  value of the six mica schists as an endmember (Q-314), suggests that at least  $>60\%$  of sedimentary component is required to produce the Mg isotopic compositions of most eclogites (Fig. 5), such that the eclogites would have anomalously high  $\text{SiO}_2$  contents ( $>55$  wt.%). In addition, the  $\text{SiO}_2$  of eclogites

does not correlate with neither  $^{87}\text{Sr}/^{86}\text{Sr}_{320\text{Ma}}$  nor  $\epsilon\text{Nd}(t)$  (Supplementary Fig. S3), further supporting that binary mixing between basalt (or eclogite) and sediment (or metasediment) might not be the case. Magnesium is fluid-mobile, thus, processes like ancient seawater alteration, prograde metamorphism (*e.g.*, release of Mg into metamorphic fluids and eclogite-host isotopic exchanges), and retrograde fluid-rock interactions (*e.g.*, interaction with metamorphic fluid during exhumation), could potentially account for the observed Mg isotopic variations. Next, we endeavor to explore how Mg isotopes behave during these processes, based on which, we highlight the importance of subduction channel fluids in generating Mg isotopic variations in exhumed eclogites.

#### *5.2.1 Seafloor alteration cannot explain the Mg isotopic signatures*

Seafloor alteration produces even larger Mg isotopic variations, with Mg isotopes likely fractionated in a different manner from that observed in the eclogites, as shown in Fig. 5. Altered oceanic crusts (AOC) from two different sites have been reported for Mg isotopic compositions (Huang et al., 2015; Teng, 2017). Carbonate-barren AOC samples recovered from IODP site 1256 in the eastern equatorial Pacific retain a mantle-like  $\delta^{26}\text{Mg}$  value as for fresh oceanic basalts (Fig. 5; Huang et al., 2015), based on which Huang et al. (2015) concluded that seafloor alteration causes limited Mg isotope fractionation, regardless of alteration temperature and water/rock ratio. At the other site (ODP site 801) in western Pacific, extensively altered AOC samples have highly variable  $\delta^{26}\text{Mg}$  values ranging from -2.76 to +0.21 (Fig. 5), with low  $\delta^{26}\text{Mg}$  values being associated with carbonate enriched samples and high  $\delta^{26}\text{Mg}$  values associated with clay-rich samples (Teng, 2017). Due to

carbonate dilution effect (Tipper et al., 2006), the AOC samples from ODP site 801 are distributed in a trend in which  $\delta^{26}\text{Mg}$  values decrease as MgO decreases (Fig. 5). Different from AOC, none of the studied eclogites (32 in total) show enrichment of light Mg isotopes, although they contain variable abundances of carbonate minerals. Furthermore, neither heavily nor less altered AOC could account for the roughly negative correlation between  $\delta^{26}\text{Mg}$  and MgO for the eclogites (Fig. 5). Thus, ancient seawater alteration is unlikely to be the cause of the variable and systemically heavier Mg isotopic compositions of the eclogites.

#### *5.2.2 The role of prograde metamorphic dehydration and eclogite-host isotopic exchange*

Magnesium isotope fractionation during prograde metamorphic dehydration or eclogite-host isotopic exchange cannot account for the Mg isotopic variations in our eclogites. It is possible that dehydrated fluids have distinct Mg isotopic compositions from the rock where the fluids are from. However, since the fraction of Mg partitioning into the fluid phases is so small compared to that inherited by metamorphic minerals during prograde metamorphism, metamorphic dehydration causes insignificant Mg isotope fractionation ( $< \pm 0.07$ ) on a bulk-rock scale (Li et al., 2011b, 2014; Teng et al., 2013; Wang et al., 2014b, 2015a, b). Local isotopic exchange between eclogite and its host rock can potentially change the original mantle-like Mg isotopic compositions of the eclogites (Wang et al., 2014a). To which direction the Mg isotopes of the eclogites fractionate depends on the types of host rock. For example, eclogite-host isotopic exchange would make eclogite boudins in carbonates/marbles isotopically lighter, whereas those enclosed in mica schists heavier (Wang et al., 2014a). However, no systemic relationship between  $\delta^{26}\text{Mg}$  and host rock type

was observed for the southwestern Tianshan eclogites. On the opposite, the carbonated eclogites (those enclosed in marbles) in our study are enriched in heavy Mg isotopes ( $\delta^{26}\text{Mg} = -0.28$  to  $+0.02$ ; Table 2), which we interpret below as a result of infiltration of external fluids derived from metasediments.

### *5.2.3 Response of Mg isotopic systematics in the eclogites to fluid-rock interactions.*

Thus, our favored interpretation of the Mg isotopic variation is fluid-rock interaction in a subduction channel. The fluids must be enriched in heavy Mg isotopes, and pervasively reactive in interacting with the eclogites because the eclogites have systemically heavier Mg isotopic compositions (Fig. 2), regardless of their diverse host rock types. Below, we discuss how the two fluid components may have affected the Mg isotopic compositions of the eclogites.

The two fluid components, due to their derivation from different hydrous minerals, have different impacts on the Mg isotopic systematics of eclogites. In the plots of  $\delta^{26}\text{Mg}$  vs.  $\text{Pb}^*$  and  $\delta^{26}\text{Mg}$  vs.  $^{87}\text{Sr}/^{86}\text{Sr}_{320\text{Ma}}$  (Fig. 6a and b), the high- $\text{Pb}^*$  and  $^{87}\text{Sr}/^{86}\text{Sr}_{320\text{Ma}}$  samples retain a mantle-like  $\delta^{26}\text{Mg}$  value, suggesting that the infiltration of high-Pb and  $^{87}\text{Sr}/^{86}\text{Sr}$  fluid component had limited influences on the Mg isotopic composition of eclogites. Being the dominant source of high-Pb and  $^{87}\text{Sr}/^{86}\text{Sr}$  component, the epidote-group minerals contain little Mg (*e.g.*, Guo et al., 2012), and thus the fluid dehydrated from them is unable to modify the Mg isotopic composition of the eclogites (although the exact  $\delta^{26}\text{Mg}$  value of any epidote-group mineral has not been reported so far). The low- $\text{Pb}^*$  and  $^{87}\text{Sr}/^{86}\text{Sr}_{320\text{Ma}}$  samples, on the other hand, have variably high  $\delta^{26}\text{Mg}$  values (Fig. 6a and b). As expected, eclogites

with high-Rb/Sr and Ba/Pb ratios have high  $\delta^{26}\text{Mg}$  values (Fig. 6c and d). Because of the complexity of the fluid system and the uncertainty of its Mg concentration and Mg isotopic composition, we are not expecting to see good correlations between  $\delta^{26}\text{Mg}$  and indices of enrichment of LILEs (such as Rb/Sr and Ba/Pb). However, the general patterns shown in Fig. 6c and d suggest that the high-LILEs component carries a significant amount of isotopically heavy Mg that has elevated the  $\delta^{26}\text{Mg}$  values of the eclogites. Mica-group minerals, as the major source of high-LILE component, are enriched in MgO, and in addition their  $\delta^{26}\text{Mg}$  values are characteristically high. For instance, biotites in metapelites from the Ivrea Zone in NW Italy have  $\delta^{26}\text{Mg}$  values ranging from -0.08 to +1.10 (Wang et al., 2015b), and phengites in eclogites from the Dabie orogen have  $\delta^{26}\text{Mg}$  values of +0.30 to +0.59 (Li et al., 2011b). Therefore, eclogites metasomatized by the mica-derived fluid could gain high- $\delta^{26}\text{Mg}$  signatures. It is also important to note that in Fig. 6c and d, a part of low-Rb/Sr and Ba/Pb samples has slightly high  $\delta^{26}\text{Mg}$  value, which we interpret as the possible influence of the talc-derived fluid, as the talc in serpentinite is depleted in LILEs but enriched in heavy Mg ( $\delta^{26}\text{Mg} = +0.06$  to  $+0.30$ ; Beinlich et al., 2014). Without good constraints on the Mg isotopic composition of fluid and the partition coefficient of MgO between fluid and eclogite, it is not yet possible to give a perfect fluid-rock interaction model for the whole dataset of the eclogites. However, the rough negative correlation between  $\delta^{26}\text{Mg}$  and MgO for the eclogites can be generally modeled as interactions of eclogites with high-MgO (*e.g.*, dehydrated from mica-group minerals or talc) and low-MgO fluid components (*e.g.*, dehydrated from epidote-group minerals) under a variety of water/rock (fluid/eclogite) ratios (Fig. 5).

### 5.3 The origins of isotopically heavy fluids in subduction channel



Fluids in subduction channels are likely to have heavy Mg isotopic compositions, although different subducted lithologies themselves show highly variable  $\delta^{26}\text{Mg}$  values. The subducted abyssal peridotites have slightly high  $\delta^{26}\text{Mg}$  values of -0.25 - +0.10 (Liu et al., 2017). The subducted sediments and altered oceanic crusts have large variations in  $\delta^{26}\text{Mg}$  values (-2.76 ‰ to +0.92 ‰), with low  $\delta^{26}\text{Mg}$  associated with carbonated rocks and with high  $\delta^{26}\text{Mg}$  associated with carbonate-free rocks (Li et al., 2010; Wang et al., 2015a; Huang et al., 2015; Teng et al., 2016; Hu et al., 2017; Teng, 2017). One might expect that subsolidus decarbonation or carbonate dissolution during metamorphism could release light Mg isotopes, making the sediment-derived fluids isotopically light. However, decarbonation is an inefficient process for carbonated sediments/basalts along the P-T paths of oceanic subduction (Gorman et al., 2006; Dasgupta and Hirschmann, 2010). Carbonate species dissolved in metamorphic fluid is thought to be mainly  $\text{CaCO}_3$  (Ague and Nicolescu, 2014; Kelemen and Manning, 2015; Li et al., 2017). Therefore, the presence of carbonate minerals in subducted rocks has negligible influence on the Mg isotopic composition of dehydrated fluids (Li et al., 2017). By contrast, breakdown of hydrous minerals might control the Mg concentration and Mg isotopic composition of dehydrated fluids. Reported  $\delta^{26}\text{Mg}$  values for Mg-rich hydrous minerals, such like mica-group minerals and talc, are higher than the normal mantle value (Li et al., 2011b; Beinlich et al., 2014; Wang et al., 2015b), and thus it is very likely that the dehydrated fluids are enriched in heavy Mg isotopes. For example, a recent study suggested that the fluid derived from talc and antigorite in serpentinite is likely characterized by high-Mg and high- $\delta^{26}\text{Mg}$ , and could be responsible for the high  $\delta^{26}\text{Mg}$  values of white schists in Western Alps (Chen et al., 2016).

## 5.4 Implications on Mg isotopic systematics in sub-arc peridotites

Fluids in subduction channels can infiltrate the mantle wedge, inducing fluid-peridotite interactions and potentially modifying the Mg isotopic composition of associated peridotites. Only a few Mg isotopic data have been reported so far for mantle wedge peridotites, and they are indeed enriched in heavy Mg isotopes: six arc peridotites from Avacha Volcano in Kamchatka analyzed by Pogge von Strandmann et al. (2011) have  $\delta^{26}\text{Mg}$  values ranging from -0.25 to -0.06, higher than the normal mantle value ( $-0.25 \pm 0.07$ ; Teng et al., 2010). Although the actual mechanism responsible for the Mg isotopic variations in these peridotites is still uncertain, their high  $\delta^{26}\text{Mg}$  values are consistent with petrological and geochemical evidence suggesting that these peridotites have been affected by upward fluid migration from the subducting slab (Ionov and Seitz, 2008). Most recently, Li et al. (2017) found that island arc or back arc basin basalts from circum-Pacific arcs, including Kamchatka, Philippines, Costa Rica and Lau Basin have generally high  $\delta^{26}\text{Mg}$  values ranging from -0.35 to +0.06. Teng et al. (2016) reported the Martinique arc lava  $\delta^{26}\text{Mg}$  values of -0.25 to -0.10. Those values overlap the Avacha peridotites and are systemically higher than normal oceanic basalts and peridotites, consistent with the interpretation that isotopically heavy fluids released from the subducted slab incorporate into the mantle wedge (Teng et al., 2016; Li et al., 2017). All the three cases suggest that massive flux of dehydrated fluid into the sub-arc mantle could facilitate extensive fluid-peridotite interaction and shift the  $\delta^{26}\text{Mg}$  of sub-arc peridotite towards higher values.

## 6. Conclusions

To reveal the nature of fluid-rock interactions in subduction channels and the influence of subduction-zone fluids on the Mg isotopic systematics in exhumed rocks, we present major and trace elements, and Sr-Nd-Mg isotopic data for the eclogites and mica schists from southwestern Tianshan, China. The following conclusions can be drawn:

(1) The eclogites have high Ba/Rb and Ba/K but low Ce/Pb ratios, suggesting the overprint of subduction-zone metamorphic metasomatism. The highly radiogenic Sr isotopic composition ( $^{87}\text{Sr}/^{86}\text{Sr}_{320\text{Ma}} = 0.7058\text{--}0.7117$ ; higher than that of coeval seawater), together with the varying and mostly low Ni and Co concentrations, further indicate that the eclogites have interacted with fluids mainly released from subducted sediments, with limited contributions from altered oceanic crust- or serpentinite-derived fluids.

(2) The positive correlation between  $^{87}\text{Sr}/^{86}\text{Sr}$  and  $\text{Pb}^*$ , and the bidirectional patterns in  $^{87}\text{Sr}/^{86}\text{Sr}$  - Rb/Sr,  $\text{Pb}^*$  - Rb/Sr, and  $\text{Pb}^*$  - Ba/Pb spaces, suggest interaction of the eclogites with compositionally different two fluid components: the high-LILEs component which could be derived from dehydration of mica-group minerals, and the high-Pb and  $^{87}\text{Sr}/^{86}\text{Sr}$  component likely released from epidote-group minerals in subducted sediments.

(3) The highly variable and systemically heavy Mg isotopic compositions of eclogites ( $\delta^{26}\text{Mg} = -0.37$  to  $+0.26$  ‰) resulted from fluid-rock interactions in the subduction channel. The high-LILE component, dehydrated from Mg-rich mica-group minerals or to a less extent from talc, contains a considerable amount of Mg that has shifted the  $\delta^{26}\text{Mg}$  of the eclogites towards higher values. The high-Pb and  $^{87}\text{Sr}/^{86}\text{Sr}$

component, dehydrated from Mg-poor epidote-group minerals, has little Mg so as not to influence the Mg isotopic composition of the eclogites.

## Acknowledgement

The authors would like to thank two anonymous reviewers for insightful comments and Editor Sun-Lin Chung for careful and efficient handling. This study was financially supported by National Natural Science Foundation of China (41230209) to SGL, National Science Foundation (EAR-1340160) to FZT, and National Science Foundation of China (Grants 41330210, 41520104004) and Major State Basic Research Development Program (Grant 2015CB856105) to LFZ.

## Reference

- Agard, P., Yamato, P., Jolivet, L. and Burov, E. (2009) Exhumation of oceanic blueschists and eclogites in subduction zones: timing and mechanisms. *Earth-Science Reviews* 92, 53-79.
- Ague, J.J. and Nicolescu, S. (2014) Carbon dioxide released from subduction zones by fluid-mediated reactions. *Nature Geoscience* 7, 355-360.
- Ai, Y.L., Zhang, L.F., Li, X.P., Qu, J.F., (2006) Geochemical characteristics and tectonic implications of HP-UHP eclogites and blueschists in southwestern Tianshan, China. *Progress in Natural Science* 16, 624-632.
- Bebout, G.E. (2007) Metamorphic chemical geodynamics of subduction zones. *Earth and Planetary Science Letters* 260, 373-393.
- Bebout, G.E., Agard, P., Kobayashi, K., Moriguti, T. and Nakamura, E. (2013) Devolatilization history and trace element mobility in deeply subducted sedimentary rocks: Evidence from Western Alps HP/UHP suites. *Chemical Geology* 342, 1-20.
- Bebout, G.E., Bebout, A.E. and Graham, C.M. (2007) Cycling of B, Li, and LILE (K, Cs, Rb, Ba, Sr) into subduction zones: SIMS evidence from micas in high-P/T metasedimentary rocks. *Chemical Geology* 239, 284-304.
- Bebout, G.E. and Penniston-Dorland, S.C. (2016) Fluid and mass transfer at subduction interfaces—The field metamorphic record. *Lithos* 240–243, 228-258.

470 Beinlich, A., Klemm, R., John, T. and Gao, J. (2010) Trace-element mobilization during  
471 Ca-metasomatism along a major fluid conduit: Eclogitization of blueschist as a consequence  
472 of fluid–rock interaction. *Geochimica et Cosmochimica Acta* 74, 1892-1922.

473 Beinlich, A., Mavromatis, V., Austrheim, H. and Oelkers, E.H. (2014) Inter-mineral Mg  
474 isotope fractionation during hydrothermal ultramafic rock alteration-Implications for the  
475 global Mg-cycle. *Earth and Planetary Science Letters* 392, 166-176.

476 Busigny, V., Cartigny, P., Philippot, P., Ader, M. and Javoy, M. (2003) Massive recycling of  
477 nitrogen and other fluid-mobile elements (K, Rb, Cs, H) in a cold slab environment: evidence  
478 from HP to UHP oceanic metasediments of the Schistes Lustrés nappe (western Alps,  
479 Europe). *Earth and Planetary Science Letters* 215, 27-42.

480 Carswell, D.A. (1990) Eclogite facies rocks. Blackie and Son Ltd, pp 14-49.

481 Chen, Y.-X., Schertl, H.P., Zheng, Y.-F., Huang, F., Zhou, K. and Gong, Y.-Z. (2016) Mg-O  
482 isotopes trace the origin of Mg-rich fluids in the deeply subducted continental crust of  
483 Western Alps. *Earth and Planetary Science Letters* 456, 157-167..

484 Chu, Z., Chen, F., Yang, Y. and Guo, J. (2009) Precise determination of Sm, Nd  
485 concentrations and Nd isotopic compositions at the nanogram level in geological samples by  
486 thermal ionization mass spectrometry. *Journal of Analytical Atomic Spectrometry* 24,  
487 1534-1544.

488 Dasgupta, R. and Hirschmann, M.M. (2010) The deep carbon cycle and melting in Earth's  
489 interior. *Earth and Planetary Science Letters* 298, 1-13.

490 Du, J.-X., Zhang, L.-F., Shen, X.-J. and Bader, T. (2014a) A new PTt path of eclogites from  
491 Chinese southwestern Tianshan: constraints from PT pseudosections and Sm-Nd isochron  
492 dating. *Lithos* 200, 258-272.

493 Du, J., Zhang, L., Bader, T., Chen, Z. and Lü, Z. (2014b) Metamorphic evolution of relict  
494 lawsonite- bearing eclogites from the (U) HP metamorphic belt in the Chinese southwestern  
495 Tianshan. *Journal of Metamorphic Geology* 32, 575-598.

496 Du, J., Zhang, L., Lü, Z. and Chu, X. (2011) Lawsonite-bearing chloritoid–glaucophane  
497 schist from SW Tianshan, China: phase equilibria and P–T path. *Journal of Asian Earth*  
498 *Sciences* 42, 684-693.

499 Foster G L, Pogge von Strandmann P A E. and Rae J W B. (2010) Boron and magnesium  
500 isotopic composition of seawater. *Geochemistry, Geophysics, Geosystems* 11(8),  
501 DOI: 10.1029/2010GC003201.

502 Gao, J., John, T., Klemm, R. and Xiong, X. (2007) Mobilization of Ti–Nb–Ta during  
503 subduction: evidence from rutile-bearing dehydration segregations and veins hosted in  
504 eclogite, Tianshan, NW China. *Geochimica et Cosmochimica Acta* 71, 4974-4996.

505 Gao, J. and Klemm, R. (2001) Primary fluids entrapped at blueschist to eclogite transition:  
506 evidence from the Tianshan meta-subduction complex in northwestern China. *Contributions*  
507 *to Mineralogy and Petrology* 142, 1-14.

508 Gao, J. and Klemmd, R. (2003) Formation of HP–LT rocks and their tectonic implications in  
509 the western Tianshan Orogen, NW China: geochemical and age constraints. *Lithos* 66, 1-22.

510 Gao, J., Klemmd, R., Zhang, L., Wang, Z. and Xiao, X. (1999) PT path of  
511 high-pressure/low-temperature rocks and tectonic implications in the western Tianshan  
512 Mountains, NW China. *Journal of Metamorphic Geology* 17, 621-636.

513 Gao, S., Zhang, B.-R., Gu, X.-M., Xie, Q.-L., Gao, C.-L. and Guo, X.-M. (1995)  
514 Silurian-Devonian provenance changes of South Qinling basins: implications for accretion of  
515 the Yangtze (South China) to the North China cratons. *Tectonophysics* 250, 183-197.

516 Gerya, T.V., Stöckhert, B. and Perchuk, A.L. (2002) Exhumation of high- pressure  
517 metamorphic rocks in a subduction channel: A numerical simulation. *Tectonics* 21, 6-1-6-19.

518 Glodny, J., Austrheim, H., Molina, J.F., Rusin, A.I. and Seward, D. (2003) Rb/Sr record of  
519 fluid-rock interaction in eclogites: The Marun-Keu complex, Polar Urals, Russia. *Geochimica  
520 et Cosmochimica Acta* 67, 4353-4371.

521 Gorman, P.J., Kerrick, D. and Connolly, J. (2006) Modeling open system metamorphic  
522 decarbonation of subducting slabs. *Geochemistry, Geophysics, Geosystems* 7.

523 Guo, S., Ye, K., Chen, Y., Liu, J.-B., Mao, Q. and Ma, Y.-G. (2012) Fluid-rock interaction  
524 and element mobilization in UHP metabasalt: Constraints from an omphacite-epidote vein  
525 and host eclogites in the Dabie orogen. *Lithos* 136-139, 145-167.

526 Halama, R., John, T., Herms, P., Hauß, F. and Schenk, V. (2011) A stable (Li, O) and  
527 radiogenic (Sr, Nd) isotope perspective on metasomatic processes in a subducting slab.  
528 *Chemical Geology* 281, 151-166.

529 Horodyskyj, U., Lee, C.-T.A. and Luffi, P. (2009) Geochemical evidence for exhumation of  
530 eclogite via serpentinite channels in ocean-continent subduction zones. *Geosphere* 5,  
531 426-438.

532 Hu, Y., Teng, F. -Z, Plank, T. and Huang, H.-J. (2017) Magnesium isotopic composition of  
533 subducting marine sediments. *Chemical Geology*,  
534 <http://dx.doi.org/10.1016/j.chemgeo.2017.06.010>

535 Huang, F., Chen, L., Wu, Z. and Wang, W. (2013) First-principles calculations of equilibrium  
536 Mg isotope fractionations between garnet, clinopyroxene, orthopyroxene, and olivine:  
537 Implications for Mg isotope thermometry. *Earth and Planetary Science Letters* 367, 61-70.

538 Huang, J., Ke, S., Gao, Y., Xiao, Y. and Li, S. (2015) Magnesium isotopic compositions of  
539 altered oceanic basalts and gabbros from IODP site 1256 at the East Pacific Rise. *Lithos* 231,  
540 53-61.

541 Ionov, D.A. and Seitz, H.-M. (2008) Lithium abundances and isotopic compositions in  
542 mantle xenoliths from subduction and intra-plate settings: mantle sources vs. eruption  
543 histories. *Earth and Planetary Science Letters* 266, 316-331.

544 John, T., Gussone, N., Podladchikov, Y.Y., Bebout, G.E., Dohmen, R., Halama, R., Klemm,  
545 R., Magna, T. and Seitz, H.-M. (2012) Volcanic arcs fed by rapid pulsed fluid flow through  
546 subducting slabs. *Nature Geoscience* 5, 489-492.

547 John, T., Klemm, R., Gao, J. and Garbe-Schönberg, C.-D. (2008) Trace-element mobilization  
548 in slabs due to non steady-state fluid–rock interaction: constraints from an eclogite-facies  
549 transport vein in blueschist (Tianshan, China). *Lithos* 103, 1-24.

550 John, T., Scherer, E.E., Haase, K. and Schenk, V. (2004) Trace element fractionation during  
551 fluid-induced eclogitization in a subducting slab: trace element and Lu–Hf–Sm–Nd isotope  
552 systematics. *Earth and Planetary Science Letters* 227, 441-456.

553 Kelemen, P.B. and Manning, C.E. (2015) Reevaluating carbon fluxes in subduction zones,  
554 what goes down, mostly comes up. *Proceedings of the National Academy of Sciences* 112,  
555 E3997-E4006.

556 Kelley, K.A., Plank, T., Ludden, J. and Staudigel, H. (2003) Composition of altered oceanic  
557 crust at ODP Sites 801 and 1149. *Geochemistry, Geophysics, Geosystems* 4, 890, doi:  
558 10.1029/2002GC000435.

559 Kessel, R., Schmidt, M.W., Ulmer, P. and Pettke, T. (2005) Trace element signature of  
560 subduction-zone fluids, melts and supercritical liquids at 120-180 km depth. *Nature* 437,  
561 724-727.

562 King, R.L., Bebout, G.E., Moriguti, T. and Nakamura, E. (2006) Elemental mixing  
563 systematics and Sr–Nd isotope geochemistry of mélange formation: obstacles to  
564 identification of fluid sources to arc volcanics. *Earth and Planetary Science Letters* 246,  
565 288-304.

566 Klemm, R. (2013) *Metasomatism During High-Pressure Metamorphism: Eclogites and*  
567 *Blueschist-Facies Rocks, Metasomatism and the Chemical Transformation of Rock*. Springer,  
568 pp. 351-413.

569 Klemm, R., John, T., Scherer, E., Rondenay, S. and Gao, J. (2011) Changes in dip of  
570 subducted slabs at depth: petrological and geochronological evidence from HP–UHP rocks  
571 (Tianshan, NW-China). *Earth and Planetary Science Letters* 310, 9-20.

572 Lü, Z., Zhang, L., Du, J. and Bucher, K. (2009) Petrology of coesite- bearing eclogite from  
573 Habutengsu Valley, western Tianshan, NW China and its tectonometamorphic implication.  
574 *Journal of Metamorphic Geology* 27, 773-787.

575 Lü, Z., Zhang, L., Du, J., Yang, X., Tian, Z. and Xia, B. (2012) Petrology of HP metamorphic  
576 veins in coesite-bearing eclogite from western Tianshan, China: fluid processes and  
577 elemental mobility during exhumation in a cold subduction zone. *Lithos* 136, 168-186.

578 Li, J.-L., Klemm, R., Gao, J. and John, T. (2016a) Poly-cyclic Metamorphic Evolution of  
579 Eclogite: Evidence for Multistage Burial–Exhumation Cycling in a Subduction Channel.  
580 *Journal of Petrology* 57, 119-146.

581 Li, Q.-L., Lin, W., Su, W., Li, X.-h., Shi, Y.-H., Liu, Y. and Tang, G.-Q. (2011a) SIMS U–Pb  
582 rutile age of low-temperature eclogites from southwestern Chinese Tianshan, NW China.  
583 *Lithos* 122, 76-86.

584 Li, S.-G, Yang, W., Ke, S., Meng, X.-N, Tian, H.-C., Xu, L.-J., He, Y.-S., Huang, J., Wang,  
585 X.-C., Xia, Q.-K., Sun, W.-D., Yang, X.-Y., Ren, Z.-Y., Wei, H.-Q., Liu, Y.-S., Meng, F.-C.  
586 and Yan, J. (2017) Deep carbon cycles constrained by a large-scale mantle Mg isotope  
587 anomaly in eastern China. *National Science Review* 4, 111-120.

588 Li, W.-Y., Teng, F.-Z., Ke, S., Rudnick, R.L., Gao, S., Wu, F.-Y. and Chappell, B. (2010)  
589 Heterogeneous magnesium isotopic composition of the upper continental crust. *Geochimica*  
590 *et Cosmochimica Acta* 74, 6867-6884.

591 Li, W.-Y., Teng, F.-Z., Xiao, Y. and Huang, J. (2011b) High-temperature inter-mineral  
592 magnesium isotope fractionation in eclogite from the Dabie orogen, China. *Earth and*  
593 *Planetary Science Letters* 304, 224-230.

594 Li, W.Y., Teng, F.Z., Wing, B.A. and Xiao, Y. (2014) Limited magnesium isotope  
595 fractionation during metamorphic dehydration in metapelites from the Onawa contact  
596 aureole, Maine. *Geochemistry, Geophysics, Geosystems* 15, 408-415.

597 Li, W. Y., Teng, F. Z., Xiao, Y., Gu, H. O., Zha, X. P. and Huang, J. (2016b) Empirical  
598 calibration of the clinopyroxene–garnet magnesium isotope geothermometer and  
599 implications. *Contributions to Mineralogy and Petrology* 171(7), 1-14.

600 Ling M X, Sedaghatpour F, Teng F Z., Hays, P.D., Strauss, J. and Sun, W.D. (2011)  
601 Homogeneous magnesium isotopic composition of seawater: an excellent geostandard for Mg  
602 isotope analysis. *Rapid Communications in Mass Spectrometry* 25(19): 2828-2836.

603 Liu, P.-P., Teng, F.-Z., Dick, HJB., Zhou M.-F. and Chung, S.-L (2017) Magnesium isotopic  
604 composition of the oceanic mantle and oceanic Mg cycling. *Geochimica et Cosmochimica*  
605 *Acta* 206, 151-165.

606 Miller, C., Stosch, H.-G. and Hoernes, S. (1988) Geochemistry and origin of eclogites from  
607 the type locality Koralpe and Saualpe, Eastern Alps, Austria. *Chemical Geology* 67, 103-118.

608 Plank, T. and Langmuir, C.H. (1998) The chemical composition of subducting sediment and  
609 its consequences for the crust and mantle. *Chemical geology* 145, 325-394.

610 Pogge von Strandmann, P.A.E., Elliott, T., Marschall, H.R., Coath, C., Lai, Y.-J., Jeffcoate,  
611 A.B. and Ionov, D.A. (2011) Variations of Li and Mg isotope ratios in bulk chondrites and  
612 mantle xenoliths. *Geochimica et Cosmochimica Acta* 75, 5247-5268.

613 Poli S. and Schmidt, M.W. (2002) Petrology of subducted slabs. *Annual Review of Earth and*  
614 *Planetary Sciences* 30, 207-235.

615 Pogge von Strandmann, P.A.P., Dohmen, R., Marschall, H.R., Schumacher, J.C. and Elliott,  
616 T. (2015) Extreme magnesium isotope fractionation at outcrop scale records the mechanism  
617 and rate at which reaction fronts advance. *Journal of Petrology* 56, 33-58.



618 Simons, K.K., Harlow, G.E., Brueckner, H.K., Goldstein, S.L., Sorensen, S.S., Hemming,  
619 N.G. and Langmuir, C.H. (2010) Lithium isotopes in Guatemalan and Franciscan HP–LT  
620 rocks: Insights into the role of sediment-derived fluids during subduction. *Geochimica et*  
621 *Cosmochimica Acta* 74, 3621-3641.

622 Su, W., Gao, J., Klemd, R., Li, J.-L., Zhang, X., Li, X.-H., Chen, N.-S. and Zhang, L. (2010)  
623 U–Pb zircon geochronology of Tianshan eclogites in NW China: implication for the collision  
624 between the Yili and Tarim blocks of the southwestern Altaids. *European Journal of*  
625 *Mineralogy* 22, 473-478.

626 Sun, S.-S. and McDonough, W. (1989) Chemical and isotopic systematics of oceanic basalts:  
627 implications for mantle composition and processes. Geological Society, London, Special  
628 Publications 42, 313-345.

629 Teng, F.-Z. (2017) Magnesium isotope geochemistry. *Reviews in Mineralogy &*  
630 *Geochemistry* 82, 219-287.

631 Teng, F.-Z., Hu, Y. and Chauvel, C. (2016) Magnesium isotope geochemistry in arc  
632 volcanism. *Proceedings of the National Academy of Sciences*, 201518456.

633 Teng, F.-Z., Li, W.-Y., Ke, S., Marty, B., Dauphas, N., Huang, S., Wu, F.-Y. and Pourmand,  
634 A. (2010) Magnesium isotopic composition of the Earth and chondrites. *Geochimica et*  
635 *Cosmochimica Acta* 74, 4150-4166.

636 Teng F. -Z., Li W. Y., Ke S., Yang W., Liu S. A., Sedaghatpour F., Wang S. J., Huang K. J.,  
637 Hu Y., Ling M. X., Xiao Y., Liu X. M., Li X. W., Gu H. O., Sio C., Wallace D., Su B. X.,  
638 Zhao L., Harrington M. and Brewer A. (2015) Magnesium isotopic compositions of  
639 international geological reference materials. *Geostandards and Geoanalytical Research* 39,  
640 329-339.

641 Teng, F.-Z., Wadhwa, M. and Helz, R.T. (2007) Investigation of magnesium isotope  
642 fractionation during basalt differentiation: implications for a chondritic composition of the  
643 terrestrial mantle. *Earth and Planetary Science Letters* 261, 84-92.

644 Teng, F.Z. and Yang, W. (2014) Comparison of factors affecting the accuracy of  
645 high- precision magnesium isotope analysis by multi- collector inductively coupled plasma  
646 mass spectrometry. *Rapid Communications in Mass Spectrometry* 28, 19-24.

647 Teng, F.Z., Yang, W., Rudnick, R.L. and Hu, Y. (2013) Heterogeneous magnesium isotopic  
648 composition of the lower continental crust: A xenolith perspective. *Geochemistry,*  
649 *Geophysics, Geosystems* 14, 3844-3856.

650 Tipper, E., Galy, A., Gaillardet, J., Bickle, M., Elderfield, H. and Carder, E. (2006) The  
651 magnesium isotope budget of the modern ocean: Constraints from riverine magnesium  
652 isotope ratios. *Earth and Planetary Science Letters* 250, 241-253.

653 van der Straaten, F., Halama, R., John, T., Schenk, V., Hauff, F. and Andersen, N. (2012)  
654 Tracing the effects of high-pressure metasomatic fluids and seawater alteration in  
655 blueschist-facies overprinted eclogites: Implications for subduction channel processes.  
656 *Chemical Geology* 292, 69-87.

657 van der Straaten, F., Schenk, V., John, T. and Gao, J. (2008) Blueschist-facies rehydration of  
658 eclogites (Tian Shan, NW-China): implications for fluid–rock interaction in the subduction  
659 channel. *Chemical Geology* 255, 195-219.

660 Veizer, J. (1989) Strontium isotopes in seawater through time. *Annual Review of Earth and*  
661 *Planetary Sciences* 17, 141-167.

662 Wang, S.-J., Teng, F.-Z. and Li, S.-G. (2014a) Tracing carbonate–silicate interaction during  
663 subduction using magnesium and oxygen isotopes. *Nature communications* 5.

664 Wang, S.-J., Teng, F.-Z., Li, S.-G. and Hong, J.-A. (2014b) Magnesium isotopic systematics  
665 of mafic rocks during continental subduction. *Geochimica et Cosmochimica Acta* 143, 34-48.

666 Wang, S.-J., Teng, F.-Z., Rudnick, R.L. and Li, S.-G. (2015a) The behavior of magnesium  
667 isotopes in low-grade metamorphosed mudrocks. *Geochimica et Cosmochimica Acta* 165,  
668 435-448.

669 Wang, S.-J., Teng, F.-Z. and Bea, F. (2015b) Magnesium isotopic systematics of metapelite  
670 in the deep crust and implications for granite petrogenesis. *Geochem. Perspect. Lett* 1, 75-83.

671 Wang, S.-J., Teng, F.-Z. and Scott, J. (2016) Tracing the origin of continental HIMU-like  
672 intraplate volcanism using magnesium isotope systematics. *Geochimica et Cosmochimica*  
673 *Acta* 185, 78-87.

674 Windley, B., Allen, M., Zhang, C., Zhao, Z. and Wang, G. (1990) Paleozoic accretion and  
675 Cenozoic reformation of the Chinese Tien Shan range, central Asia. *Geology* 18, 128-131.

676 Xiao, Y., Lavis, S., Niu, Y., Pearce, J.A., Li, H., Wang, H. and Davidson, J. (2012)  
677 Trace-element transport during subduction-zone ultrahigh-pressure metamorphism: Evidence  
678 from western Tianshan, China. *Geological Society of America Bulletin* 124, 1113-1129.

679 Yang, W., Teng, F.-Z. and Zhang, H.-F. (2009) Chondritic magnesium isotopic composition  
680 of the terrestrial mantle: a case study of peridotite xenoliths from the North China craton.  
681 *Earth and Planetary Science Letters* 288, 475-482.

682 Yang, X., Zhang, L.F., Tian, Z.L., Bader, T., (2013) Petrology and U-Pb zircon dating of  
683 coesite-bearing metapelites from the Kebuerte Valley, western Tianshan, China. *Journal of*  
684 *Asian Earth Sciences* 70-71, 295-307.

685 Zack, T. and John, T. (2007) An evaluation of reactive fluid flow and trace element mobility  
686 in subducting slabs. *Chemical Geology* 239, 199-216.

687 Zhang, L., Du, J., Lü, Z., Yang, X., Gou, L., Xia, B., Chen, Z., Wei, C. and Song, S. (2013) A  
688 huge oceanic-type UHP metamorphic belt in southwestern Tianshan, China: Peak  
689 metamorphic age and PT path. *Chinese Science Bulletin* 58, 4378-4383.

690 Zhang, L., Ellis, D.J. and Jiang, W. (2002) Ultrahigh-pressure metamorphism in western  
691 Tianshan, China: Part I. Evidence from inclusions of coesite pseudomorphs in garnet and  
692 from quartz exsolution lamellae in omphacite in eclogites. *American mineralogist* 87,  
693 853-860.

694 Zhang, L-F., Ellis, D., Williams, S. and Jiang, W.-B. (2003) Ultrahigh-pressure  
 695 metamorphism in eclogites from the western Tianshan, China — Reply. *American*  
 696 *Mineralogist* 88, 1157-1160.

697 Zhang, L., Lü, Z., Zhang, G. and Song, S. (2008) The geological characteristics of  
 698 oceanic-type UHP metamorphic belts and their tectonic implications: Case studies from  
 699 Southwest Tianshan and North Qaidam in NW China. *Chinese Science Bulletin* 53,  
 700 3120-3130.

701 Zhang, L., Song, S., Liou, J.G., Ai, Y. and Li, X. (2005) Relict coesite exsolution in  
 702 omphacite from Western Tianshan eclogites, China. *American Mineralogist* 90, 181-186.

703 Zhang, L., Zhang, L., Lü, Z., Bader, T. and Chen, Z. (2016) Nb–Ta mobility and  
 704 fractionation during exhumation of UHP eclogite from southwestern Tianshan, China.  
 705 *Journal of Asian Earth Sciences* 122, 136-157.

706 Zindler, A. and Hart, S. (1986) Chemical geodynamics. *Annual review of earth and planetary*  
 707 *sciences* 14, 493-571.

708

## Figure Captions

Fig. 1: Strontium and Nd isotopic compositions of the eclogites from southwestern Tianshan. MORB and OIB fields are from Zindler and Hart (1986);  $^{87}\text{Sr}/^{86}\text{Sr}$  ratio of the Ordovician to Carboniferous (O-C) seawater is from Veizer (1989), and  $^{87}\text{Sr}/^{86}\text{Sr}$  ratio of the global subducting sediments (GLOSS) can be high as much as 0.73 (Plank and Langmuir, 1998)

Fig. 2: Histogram of  $\delta^{26}\text{Mg}$  values for the eclogites from southwestern Tianshan.  $\delta^{26}\text{Mg}$  values of the eclogites with continental origin are from Li et al. (2010) and Wang et al. (2014a, b).  $\delta^{26}\text{Mg}$  values of the unaltered oceanic crust are from Teng et al. (2010).

Fig. 3: Ba/Rb vs. K (a), K/Th vs. Ba/Th (b), and Ce/Pb vs. 1/Pb (c) diagrams to differentiate between ancient seawater alteration and metamorphic metasomatism after Bebout (2007). The Ni vs. Co diagram (d) indicates that most eclogites have lower Ni and Co concentration than oceanic basalts. Data of MORB and OIB are from Sun and McDonough (1989); the Ni and Co of average serpentinite are from data compiled by van der Straaten et al. (2008).

Fig. 4: Rb/Sr vs.  $\text{Pb}^*$  (a), Ba/Pb vs.  $\text{Pb}^*$  (b),  $^{87}\text{Sr}/^{86}\text{Sr}_{(t)}$  vs.  $\text{Pb}^*$  (c) and  $^{87}\text{Sr}/^{86}\text{Sr}_{(t)}$  vs. Rb/Sr (d) diagrams to indicate the two fluid components. The  $\text{Pb}^*$  represents an indices of enrichment of Pb in the eclogites:  $\text{Pb}^* = 2 \cdot \text{Pb}_N / (\text{Ce}_N + \text{Pr}_N)$ . The higher the  $\text{Pb}^*$ , the more enrichment of Pb for the eclogites. The carbonated eclogites are marked as dashed outline. The black

triangle in panels a and b represents the average altered oceanic crust (super composite of Ocean Drilling Program Site 801) in Kelley et al. (2003). Black square and diamond represent the composition of MORB and OIB, respectively. The component 1 is enriched in LILEs, which might be derived from dehydration of mica-group minerals. The component 2 is enriched in Pb and  $^{87}\text{Sr}/^{86}\text{Sr}$ , likely released from epidote-group minerals.

Fig. 5: The variation of  $\delta^{26}\text{Mg}$  values as a function of MgO content for the eclogites (yellow circle) and mica schists (blue diamond) from southwestern Tianshan. The compositions of altered oceanic crust (AOC) from ODP site 801 and IODP site 1256 are from Huang et al. (2015) and Teng (2017). The co-variation between  $\delta^{26}\text{Mg}$  and MgO for the eclogites can be roughly modeled as fluid-rock interactions of the eclogites with compositionally different two fluid components. We assume that the component 1, because of its origin from Mg-rich mica-group minerals or to a less extent talc, have  $\delta^{26}\text{Mg} = +1.00$  and  $\text{MgO} = 1$  wt.%; the component 2, released from Mg-poor epidote-group minerals, contain very little Mg (assuming  $\text{MgO} = 0.05$  wt.%). Although we assign a value of  $+1.00$  for the  $\delta^{26}\text{Mg}$  of the low-MgO component 2, the change of this value will not affect the modelling significantly, as the component 2 contains too little Mg so as not to influence the Mg isotopic composition of the eclogites. Thus, the two purple curves with increment of 10% represent the fluid-rock interaction of an eclogite ( $\delta^{26}\text{Mg} = -0.25$ ;  $\text{MgO} = 8$  wt.%) with high-MgO and low-MgO fluid components, with the partition coefficient of MgO between fluid and eclogite,  $D_{\text{eclogite/fluid}} = 4$ . The black dotted curve represents binary mixing between sediments and basalts, which suggests that >60% of sedimentary component is required to produce the Mg

isotopic composition of the eclogites. The green bar represents the normal mantle  $\delta^{26}\text{Mg}$  value (Teng et al., 2010).

Fig. 6:  $\delta^{26}\text{Mg}$  vs.  $\text{Pb}^*$  (a),  $\delta^{26}\text{Mg}$  vs.  $^{87}\text{Sr}/^{86}\text{Sr}_{(t)}$  (b),  $\delta^{26}\text{Mg}$  vs.  $\text{Rb}/\text{Sr}$  (c), and  $\delta^{26}\text{Mg}$  vs.  $\text{Ba}/\text{Pb}$  (d) diagrams showing the influence of the two fluid components on the Mg isotopic systematics of eclogites (shown as solid arrows). The carbonated eclogites are marked as dashed outline. The high-LILE fluid component contains a considerable amount of isotopically heavy Mg to shift the  $\delta^{26}\text{Mg}$  of eclogites towards a higher value, whereas the high- $^{87}\text{Sr}/^{86}\text{Sr}$  and -Pb fluid component contains little heavy Mg to influence the Mg isotopic systematics of eclogites. Some low-Rb/Sr and -Ba/Pb samples also have slightly heavy Mg isotopic compositions, which might point towards the contributions of fluids dehydrated from talc in serpentinite (shown as dashed arrows; Beinlich et al., 2014).

## Table Captions

Table 1. Strontium and Nd isotopic compositions of the eclogites from southwestern Tianshan.

Table 2. Magnesium isotopic compositions of the eclogites and mica schists and their mineral separates from southwestern Tianshan.

# Tracing subduction zone fluid-rock interactions using trace element and Mg-Sr-Nd isotopes

Shui-Jiong Wang<sup>1,2\*</sup>, Fang-Zhen Teng<sup>2\*</sup>, Shu-Guang Li<sup>1</sup>, Li-Fei Zhang<sup>3</sup>, Jin-Xue Du<sup>1,3</sup>, Yong-Sheng He<sup>1</sup>, Yaoling Niu<sup>4,5</sup>

<sup>1</sup> State Key Laboratory of Geological Processes and Mineral Resources, China University of Geosciences, Beijing 100083, China

<sup>2</sup> Isotope Laboratory, Department of Earth and Space Sciences, University of Washington, Seattle, WA 98195-1310, USA

<sup>3</sup> School of Earth Space Sciences, Peking University, Beijing, China

<sup>4</sup> Institute of Oceanology, Chinese Academy of Sciences, Qingdao 266071, China

<sup>5</sup> Department of Earth Sciences, Durham University, Durham DH1 3LE, UK

Abstract: 492 words

Text: 5139 words

Figure: 6

Table: 2

Revised version submitted to *Lithos* (July 29, 2017)

\*Present address: Department of Earth and Atmospheric Sciences, Indiana University, Bloomington, IN 47405 USA.

Corresponding authors: [sxw057@gmail.com](mailto:sxw057@gmail.com)(S.-J. Wang); [fteng@u.washington.edu](mailto:fteng@u.washington.edu) (F.-Z. Teng)

## Abstract

Slab-derived fluids play a key role in mass transfer and elemental/isotopic exchanges in subduction zones. The exhumation of deeply subducted crust is achieved via a subduction channel where fluids from various sources are abundant, and thus the chemical/isotopic compositions of these rocks could have been modified by subduction-zone fluid-rock interactions. Here, we investigate the Mg isotopic systematics of eclogites from southwestern Tianshan, in conjunction with major/trace element and Sr-Nd isotopes, to characterize the source and nature of fluids and to decipher how fluid-rock interactions in subduction channel might influence the Mg isotopic systematics of exhumed eclogites. The eclogites have high LILEs (especially Ba) and Pb, high initial  $^{87}\text{Sr}/^{86}\text{Sr}$  (up to 0.7117; higher than that of coeval seawater), and varying Ni and Co (mostly lower than those of oceanic basalts), suggesting that these eclogites have interacted with metamorphic fluids mainly released from subducted sediments, with minor contributions from altered oceanic crust or altered abyssal peridotites. The positive correlation between  $^{87}\text{Sr}/^{86}\text{Sr}$  and  $\text{Pb}^*$  (an index of Pb enrichment;  $\text{Pb}^* = 2 \times \text{Pb}_\text{N}/[\text{Ce}_\text{N} + \text{Pr}_\text{N}]$ ), and the decoupling relationships and bidirectional patterns in  $^{87}\text{Sr}/^{86}\text{Sr}$ -Rb/Sr,  $\text{Pb}^*$ -Rb/Sr and  $\text{Pb}^*$ -Ba/Pb spaces imply the presence of two compositionally different components for the fluids: one enriched in LILEs, and the other enriched in Pb and  $^{87}\text{Sr}/^{86}\text{Sr}$ . The systematically heavier Mg isotopic compositions ( $\delta^{26}\text{Mg} = -0.37$  to  $+0.26$ ) relative to oceanic basalts ( $-0.25 \pm 0.07$ ) and the roughly negative correlation of  $\delta^{26}\text{Mg}$  with MgO for the southwestern Tianshan eclogites, cannot be explained by inheritance of Mg isotopic signatures from ancient seafloor alteration or prograde metamorphism. Instead, the signatures are most likely produced by fluid-rock interactions during the exhumation of



eclogites. The high Rb/Sr and Ba/Pb but low Pb\* eclogites generally have high bulk-rock  $\delta^{26}\text{Mg}$  values, whereas high Pb\* and  $^{87}\text{Sr}/^{86}\text{Sr}$  eclogites have mantle-like  $\delta^{26}\text{Mg}$  values, suggesting that the two fluid components have diverse influences on the Mg isotopic systematics of these eclogites. The LILE-rich fluid component, possibly derived from mica-group minerals, contains a considerable amount of isotopically heavy Mg that has shifted the  $\delta^{26}\text{Mg}$  of the eclogites towards higher values. By contrast, the  $^{87}\text{Sr}/^{86}\text{Sr}$ - and Pb-rich fluid component, most likely released from epidote-group minerals in metasediments, has little Mg so as not to modify the Mg isotopic composition of the eclogites. In addition, the influence of talc-derived fluid might be evident in a very few eclogites that have low Rb/Sr and Ba/Pb but slightly heavier Mg isotopic compositions. These findings represent an important step toward a broad understanding of the Mg isotope geochemistry in subduction zones, and contributing to understanding why island arc basalts have averagely heavier Mg isotopic compositions than the normal mantle.

**Keywords:** Mg isotopes, subduction channel, fluid-rock interaction, eclogite, Tianshan

## 1. Introduction

Subduction channel is a highly reactive interface between subducting oceanic lithosphere and mantle wedge, in which mass transfer as well as elemental and isotopic exchanges actively occur (*e.g.*, Bebout and Penniston-Dorland, 2016). In this region, fluids released from various subducting slab lithologies (*e.g.*, sediments, altered oceanic crust, and altered abyssal peridotites) can be mixed and penetrate into exhuming rocks, inducing extensive fluid-rock interactions (Zack and John, 2007; John et al., 2008; van der Straaten et al., 2008, 2012). The fluids, when emanating from the interface into the mantle wedge, can further impart their chemical/isotopic signatures to the juxtaposed mantle rocks and associated arc volcanism.

Trace elements in conjunction with Sr-Nd-O isotopic systematics have been widely used to identify and understand fluid-rock interactions in subduction channels (Glodny et al., 2003; John et al., 2004, 2012; King et al., 2006; Halama et al., 2011). The magnesium (Mg) isotopic systematics might be a useful tracer of subduction-zone fluid-rock interactions, potentially providing insights into the source and nature of fluids. Magnesium is fluid-mobile at low temperatures, which leads to large Mg isotope fractionations as much as 7 ‰ during Earth's surface processes (Teng, 2017 and references therein). Recent studies also documented high mobility of Mg during subduction-zone metamorphism (van der Straaten et al., 2008; Horodyskyj et al., 2009; Pogge von Strandmann et al., 2015; Chen et al., 2016). Chen et al. (2016) found high  $\delta^{26}\text{Mg}$  values (up to +0.72) for white schists from Western Alps, and linked them to infiltration of Mg-rich fluids derived from dehydration of

serpentinites. Recent studies also documented generally heavier Mg isotopic compositions in arc volcanic rocks relative to normal peridotitic sources ( $\delta^{26}\text{Mg} = -0.25 \pm 0.07$ ), which were explained as the addition of heavy Mg isotopes from subducting slabs to the mantle wedge (Teng et al., 2016; Li et al., 2017). A general conclusion derived from these studies is that the subduction-zone fluids might be isotopically heavy in terms of Mg isotopes. Nevertheless, the interpretation of any Mg isotopic variations in subduction-related rocks requires the knowledge of how Mg isotopes behave in subduction channels, and how fluid-rock interactions could affect the Mg isotopic systematics of a rock.

Orogenic eclogites of seafloor protolith may be the best choice to study subduction channel processes. Oceanic crust undergoes seawater alteration prior to subduction and is, therefore, more hydrated relative to the continental crust (Miller et al., 1988). It experiences extensive dehydration together with the sediment veneer during subduction (Gerya et al., 2002). In addition, the exhumation of oceanic crust via the subduction channel proceeds at relatively slower rate (mm/yr; Agard et al., 2009). All of these allow eclogites of seafloor protolith to preserve a record of extensive fluid-rock interactions during exhumation. An increasing number of studies have shown that fluid-rock interactions can readily modify the chemical and isotopic compositions of exhumed eclogites (*e.g.*, Bebout, 2007; Xiao et al., 2012; Klemd, 2013), although how the chemical/isotopic composition shift depends on the nature and abundance of fluids with which the eclogites have interacted.

In this study, we investigate a suite of well-characterized eclogites/blueschists and mica schists from southwestern Tianshan, China. We present the first Mg isotopic data for the

orogenic eclogites of seafloor protolith, and in combination with Sr-Nd isotopic and trace elemental data, we explore the influence of subduction-zone fluid-rock interactions on the Mg isotopic systematics of eclogites. Our results show that these eclogites are variably enriched in heavy Mg isotopes, which may result from interactions of the eclogites with both high-MgO and low-MgO fluids released from different hydrous minerals in the subduction channel.

## **2. Geological settings and samples**

The high-pressure to ultrahigh-pressure (HP-UHP) metamorphic belt of Chinese southwestern Tianshan, located along the suture between the Yili and the Tarim blocks, was formed during the northward subduction of the Palaeo-South Tianshan oceanic crust beneath the Yili block (Windley et al., 1990; Gao et al., 1999; Zhang et al., 2002, 2008). The eclogites and retrograded blueschists in southwestern Tianshan occur as interlayers or lenticular bodies in mica schists, representing the relic oceanic crust that experienced subduction and exhumation in response to later continental collision. The protoliths of eclogites and associated blueschists range from MORBs to OIBs as indicated by the geochemical data and their preserved pillow structures in the field (Zhang et al., 2002, 2008; Gao and Klemd, 2003; Ai et al., 2006). The eclogites and their host rocks have experienced peak coesite-bearing eclogite-facies metamorphism at 324 ~ 312 Ma (Zhang et al., 2005; Su et al., 2010; Klemd et al., 2011; Li et al., 2011a; Yang et al., 2013), followed by a slow exhumation rate to amphibolite-facies between 320 Ma and 240 Ma (*e.g.*, Zhang et al., 2013). The peak and retrograde metamorphic temperatures estimated for the southwestern Tianshan eclogites vary

from 450 to 630 °C (*e.g.*, Du et al., 2014a, b). The retrograde metamorphic temperatures are slightly higher than the peak-eclogite facies temperatures as a result of thermal relaxation during the exhumation (*e.g.*, Zhang et al., 2013). The presence of abundant millimeter to decimeter-wide and centimeter to meter-long veins in southwestern Tianshan blueschists and eclogites indicates extensive fluid-rock interactions and fluid-mediated mass transport during crustal subduction and exhumation (Gao and Klemd, 2001; Gao et al., 2007; John et al., 2008; 2012; Beinlich et al., 2010; Lü et al., 2012).

The petrology and metamorphic evolution of the studied eclogites and mica schists have been well characterized (Zhang et al., 2003; Ai et al., 2006; Lü et al., 2009; Du et al., 2011, 2014b; Xiao et al., 2012). The eclogites consist mainly of garnet, omphacite, glaucophane, paragonite, epidote, calcite, dolomite and quartz/coesite; the mica schists are mainly composed of garnet, glaucophane, phengite, epidote, paragonite, plagioclase and quartz/coesite. A detail description of the studied eclogites and mica schists including the sample localities has been given in Supplementary Table S1.

### **3. Analytical methods**

#### **3.1 Major and trace elements**

Major elements were analyzed at the Hebei Institute of Regional Geology and Mineral Resources, China, by wavelength dispersive X-Ray fluorescence spectrometry (Gao et al., 1995). Analytical uncertainties are generally better than 1%. The H<sub>2</sub>O<sup>+</sup> and CO<sub>2</sub> were determined by gravimetric methods and potentiometry, respectively. Trace elements were analyzed using an Elan 6100 DRC ICP-MS at the CAS key laboratory of crust-material and

environments, University of Science and Technology of China, Hefei. Samples were analyzed with aliquots of USGS whole-rock standards BHVO-2, BIR-1, AGV-2 and GSP-2, which were treated as unknown. Results for the USGS standards together with the reference values are reported in Supplementary Table S2. Analytical uncertainties are better than 5% for most of the elements.

### 3.2 Strontium and Nd isotopic analysis

The Sr and Nd were separated from the matrix with cation exchange chromatography with Bio-Rad AG50W-X12 resin using the method described by Chu et al. (2009). The Sr and Nd isotopes were performed using an Isoprobe-T thermal ionization mass spectrometer (TIMS) at the State Key Laboratory of Lithospheric Evolution, Institute of Geology and Geophysics, Chinese Academy of Sciences. Measured  $^{87}\text{Sr}/^{86}\text{Sr}$  and  $^{143}\text{Nd}/^{144}\text{Nd}$  ratios were corrected for mass-fractionation using  $^{86}\text{Sr}/^{88}\text{Sr} = 0.1194$  and  $^{146}\text{Nd}/^{144}\text{Nd} = 0.7219$ , respectively. During the course of this study, standards of NBS987-Sr and jNdi-Nd give a value of  $^{87}\text{Sr}/^{86}\text{Sr} = 0.710245 \pm 20$  and  $^{143}\text{Nd}/^{144}\text{Nd} = 0.512117 \pm 10$ , respectively.

### 3.3 Magnesium isotopic analysis

Magnesium isotopic ratios were analyzed for bulk rock powders and mineral separates at the University of Washington, Seattle. The separation of Mg was achieved by cation exchange chromatography using Bio-Rad AG50W-X8 resin in 1N HNO<sub>3</sub> media (Teng et al., 2007, 2010a; 2015; Yang et al., 2009; Li et al., 2010). Two standards, Kilbourne Hole (KH) olivine and seawater, were processed together with samples for each batch of column chemistry. The Mg isotopic ratios were determined using the standard-sample bracketing

protocol on a *Nu* plasma MC-ICPMS (Teng and Yang, 2014). The blank Mg signal for  $^{24}\text{Mg}$  was  $< 10^{-4}$  V, which is negligible relative to the sample signals of 3-5 V. The KH olivine and seawater yielded average  $\delta^{26}\text{Mg}$  of  $-0.25 \pm 0.05$  and  $-0.82 \pm 0.06$ , respectively, consistent with previous reported values (Foster et al., 2010; Li et al., 2010; Teng et al., 2010; Ling et al., 2011; Wang et al., 2016)

## 4. Results

Major and trace elemental compositions of the eclogites and mica schists are summarized in Supplementary Table S3. The eclogites have  $\text{SiO}_2$  ranging from 39.82 to 52.47 wt.% and MgO ranging from 3.19 to 9.68 wt.% (Supplementary Table S3), and plot in subalkalic basalt field in Zr/Ti versus Nb/Y diagram (Supplementary Fig. S1; Pearce, 1996). The high contents of  $\text{H}_2\text{O}^+$  (0.58 to 3.38 wt.%) and  $\text{CO}_2$  (0.08 to 8.96 wt.%) are consistent with the presence of water- and/or carbon oxide-bearing minerals such as zoisite/clinozoisite and calcite/dolomite. The eclogites have variably high LILEs (*e.g.*, Ba, Rb, Cs, and K) and Pb, but low Ni and Co concentrations (Supplementary Table S3). The mica schists are felsic with  $\text{SiO}_2$  ranging from 59.53 to 76.66 wt.% and MgO ranging from 1.81 to 3.60 wt.% (Supplementary Table S3). They are characterized by variable contents of LILEs, Sr and Pb, which may be controlled by different proportions of mica-group minerals (host of LILEs) and epidote-group minerals (major host of Sr and Pb) in southwestern Tianshan metasediments (*e.g.*, Xiao et al., 2012).

The Sr and Nd isotopic compositions of the eclogites are reported in Table 1. The eclogites have positive age-corrected  $\epsilon\text{Nd}_{320\text{Ma}}$  value ranging from +2.8 to +10.1 (with one

exception of -2.4; Fig. 1). They have extremely high and variable initial Sr isotopic compositions ( $^{87}\text{Sr}/^{86}\text{Sr}_{320\text{Ma}}$ ) varying from 0.7058 to 0.7117 (Fig. 1), a range that is even higher than that of Ordovician to Carboniferous seawater ( $^{87}\text{Sr}/^{86}\text{Sr} = 0.7075 - 0.7090$ ; Veizer, 1989). As a result, the eclogites plot rightward far from the field defined by depleted MORB and OIB in  $\epsilon\text{Nd}(t) - ^{87}\text{Sr}/^{86}\text{Sr}(t)$  diagram (Fig. 1).

The  $\delta^{26}\text{Mg}$  values of southwestern Tianshan eclogites vary widely from  $-0.37 \pm 0.05$  to  $+0.26 \pm 0.04$  (Table 2), equal to or higher than unaltered oceanic basalts and eclogites of continental basalt protolith, both of which have homogeneous Mg isotopic compositions around the normal mantle value ( $-0.25 \pm 0.07$ ; Fig. 2). Garnets in southwestern Tianshan eclogites yield  $\delta^{26}\text{Mg}$  values varying from  $-1.75 \pm 0.07$  to  $-1.10 \pm 0.07$ , and omphacites have  $\delta^{26}\text{Mg}$  values ranging from  $-0.04 \pm 0.05$  to  $+0.46 \pm 0.07$  (Table 2), with corresponding inter-mineral Mg isotope fractionation ( $\Delta^{26}\text{Mg}_{\text{Cpx-Grt}} = \delta^{26}\text{Mg}_{\text{Cpx}} - \delta^{26}\text{Mg}_{\text{Grt}}$ ) in the range of 1.23 - 1.98. Temperatures estimated using garnet-clinopyroxene Mg isotope geothermometer range from 485°C to 675°C (Huang et al., 2013; Li et al., 2016b), which are in rough agreement with the peak and retrograde metamorphic temperatures for the Tianshan eclogites (e.g., Du et al., 2014a, b). Six mica schists from southwestern Tianshan have bulk  $\delta^{26}\text{Mg}$  values ranging from  $-0.11 \pm 0.05$  to  $+0.23 \pm 0.02$  (Table 2).

## 5. Discussion

The overprint of fluid-rock interactions on the southwestern Tianshan eclogites/blueschists has been confirmed by many petrological and geochemical studies (John et al., 2008; van der Straaten et al., 2008, 2012; Beinlich et al., 2010; Lü et al., 2012; Li et al.,



206 2016a; Zhang et al., 2016). Depending on the nature and abundance of fluids in a subduction  
207 channel, the initial composition of an eclogite can be altered to various degrees after  
208 fluid-rock interactions. In this section, we first focus on the trace element and Sr-Nd isotopes  
209 to characterize the source and nature of the fluids, and then decipher how fluid-rock  
210 interactions may have influenced the Mg isotopic systematics of the eclogites. Finally, we  
211 discuss the Mg isotope geochemistry of slab-derived fluids in the subduction channel and  
212 their influences on the sub-arc peridotites.

## 213 **5.1 Geochemical evidence for fluid-rock interactions**

214 Trace element and Sr-Nd isotope geochemistry suggest interactions of eclogites with  
215 metamorphic fluids. The fluids are mainly derived from subducted sediments, with limited  
216 contributions from serpentinites or altered oceanic crusts. Most eclogites are variably  
217 enriched in LILEs (*e.g.*, Ba, Cs, Rb, and K) and Pb (Fig. 3), which can be produced during  
218 either ancient seafloor alteration or subduction-zone fluid-rock interactions. Bebout (2007)  
219 documented that significant enrichments of Ba and Pb in metabasaltic rocks can be most  
220 directly associated with metasomatism because these two elements are only slightly enriched  
221 in altered oceanic basalts during seafloor alteration relative to other LILEs. The consistently  
222 high Ba/Rb, high Ba/K and low Ce/Pb of our eclogites are thus indicative of HP/UHP  
223 fluid-rock interactions rather than ancient seawater alteration (Fig. 3a, b, c). Furthermore,  
224 these eclogites have extremely high initial  $^{87}\text{Sr}/^{86}\text{Sr}$  ratio up to 0.7117 (Fig. 1), a signature  
225 that cannot be attributed to pre-subduction seawater alteration because the  
226 Ordovician-Carboniferous seawater has much lower  $^{87}\text{Sr}/^{86}\text{Sr}$  ratios of 0.7075 - 0.7090

(Veizer, 1989). The high  $^{87}\text{Sr}/^{86}\text{Sr}_{320\text{Ma}}$  ratios thus must have resulted from interactions of the eclogites with fluids during metasomatism, and the fluids might be derived from subducted sediments whose  $^{87}\text{Sr}/^{86}\text{Sr}$  ratios can be as high as 0.73 (Plank and Langmuir, 1998). In contrast to Sr isotopes, Nd isotopes appear to behave conservatively during the metasomatism (King et al., 2006). Due to the low mobility of REE during metamorphic dehydration under relatively low P-T conditions (Kessel et al., 2005), slab-derived fluids would contain too little Nd to affect the Nd isotopic systematics of eclogites (van der Straaten et al., 2012), such that the eclogites retain their depleted Nd isotopic signatures (Fig. 1). In accordance with the high  $^{87}\text{Sr}/^{86}\text{Sr}$  ratios, most eclogites contain very low concentrations of Co and Ni evolving from oceanic basalts towards the GLOSS (global subducting sediments; Fig. 3d), pointing towards again interactions of the eclogites with sediment-derived fluids. Some eclogites however have Ni and Co contents overlapping or slightly higher than oceanic basalts (Fig. 3d). This indicates the possible contributions of altered oceanic crust-derived or serpentinite-derived fluids (*e.g.*, van der Straaten et al., 2012), although subducted sediments must be the dominant source for fluids that have interacted with the eclogites.

The geochemical signatures of sediment-derived fluids might vary significantly in response to the mineralogical heterogeneity of subducting sediments. The eclogites display a series of geochemical features indicative of two compositionally different fluid components (Fig. 4). As shown in Rb/Sr vs. Pb\* (an index of enrichment of Pb;  $\text{Pb}^* = 2 \cdot \text{Pb}_\text{N}/[\text{Ce}_\text{N} + \text{Pr}_\text{N}]$ ) and Ba/Pb vs. Pb\* diagrams, the enrichment of Pb in eclogites is not always associated with the enrichment of LILEs (Fig. 4a and b). The observed decoupling patterns may indicate two major fluid components: one enriched in LILEs relative to Pb (*e.g.*, high Rb/Sr and Ba/Pb but

249 low Pb\*), and the other enriched in Pb relative to LILEs (*e.g.*, high Pb\* but low Rb/Sr or  
 250 Ba/Pb). The roughly positive correlation between Pb\* and  $^{87}\text{Sr}/^{86}\text{Sr}_{320\text{Ma}}$  (Fig. 4c), suggests  
 251 that the high-Pb component also contains a significant amount of radiogenic Sr that has  
 252 elevated the  $^{87}\text{Sr}/^{86}\text{Sr}$  value of eclogites. Some carbonated eclogites are extremely enriched in  
 253 elemental Sr but have relatively low  $^{87}\text{Sr}/^{86}\text{Sr}$  values of 0.7066 – 0.7078 (Supplementary Fig.  
 254 S2), suggesting that the surrounding marbles are not the source of high- $^{87}\text{Sr}/^{86}\text{Sr}$  fluid. Instead,  
 255 the high- $^{87}\text{Sr}/^{86}\text{Sr}$  fluid component must be sourced from other metasediments, such as mica  
 256 schists. The high-LILEs component, on the other hand, might contain too little Sr to modify  
 257 the Sr isotopic composition of eclogites, as reflected by the decoupling relationship between  
 258  $^{87}\text{Sr}/^{86}\text{Sr}_{320\text{Ma}}$  and Rb/Sr (Fig. 4d): the high-Rb/Sr eclogites display low  $^{87}\text{Sr}/^{86}\text{Sr}_{320\text{Ma}}$  values,  
 259 whereas the low-Rb/Sr samples are characterized by highly radiogenic Sr isotopic  
 260 compositions (Fig. 4d). All these observations support that the eclogites were infiltrated by  
 261 two fluid components. The distinct geochemical signatures of the two fluid components are  
 262 consistent with the fact that LILEs and Sr-Pb are hosted in different hydrous minerals in  
 263 subducted sediments: mica-group minerals are the dominant host for LILEs, whereas  
 264 epidote-group minerals (and to a less extent carbonate minerals and paragonite) are the major  
 265 host of Pb and Sr (*e.g.*, Busigny et al., 2003; Bebout et al., 2007, 2013; Xiao et al., 2012). As  
 266 a result, fluid dehydrated from mica-group minerals would have high Rb/Sr and Ba/Pb ratios,  
 267 whereas fluid released from epidote-group minerals in metasediments could be enriched in  
 268 Pb and Sr (as well as  $^{87}\text{Sr}/^{86}\text{Sr}$ ). It is possible that varying modal mineralogy in the subducted  
 269 sediments (*e.g.*, mica-group minerals are abundant in metapelites and epidote-group minerals  
 270 are abundant in greywackes) can result in decomposition of mica- and epidote-group

minerals in different proportions along the subduction P-T path and generate the two fluid components in the subduction channel. During crustal subduction, biotite is thought to be completely decomposed at  $P = 1.3\text{--}1.5$  GPa, at which the epidote-group minerals such as epidote and zoisite are still stable (Poli and Schmidt, 2002). Therefore, decomposition of biotite at the early stage during crustal subduction could release a significant amount of fluid that is enriched in LILEs. At a higher pressure above 2.5 GPa, epidote and zoisite might become unstable (Carswell, 1990; Poli and Schmidt, 2002). Metamorphic dehydration at this stage could thus release abundant Sr and Pb to the fluids. Such fluids, when released from subducting oceanic crust, would migrate upward along the subduction channel, infiltrate the exhuming eclogites and impart their distinct geochemical signatures to the eclogites via fluid-rock interactions.

## **5.2 Constraining the mechanisms of Mg isotopic variations in the eclogites**

The eclogites have varying Mg contents ( $\text{MgO} = 3.2$  to  $9.7$  wt.%) at a given  $\text{SiO}_2$  content, and more variable and systemically heavier Mg isotopic composition than fresh oceanic basalts (Fig. 5). The simplest explanation for the low MgO and high  $\delta^{26}\text{Mg}$  of eclogites is physical/mechanical mixing with a high- $\delta^{26}\text{Mg}$  sedimentary component at some point before or during the exhumation of the eclogites. However, this is very unlikely because binary mixing calculation, using the highest  $\delta^{26}\text{Mg}$  value of the six mica schists as an endmember (Q-314), suggests that at least  $>60\%$  of sedimentary component is required to produce the Mg isotopic compositions of most eclogites (Fig. 5), such that the eclogites would have anomalously high  $\text{SiO}_2$  contents ( $>55$  wt.%). In addition, the  $\text{SiO}_2$  of eclogites

does not correlate with neither  $^{87}\text{Sr}/^{86}\text{Sr}_{320\text{Ma}}$  nor  $\epsilon\text{Nd}(t)$  (Supplementary Fig. S3), further supporting that binary mixing between basalt (or eclogite) and sediment (or metasediment) might not be the case. Magnesium is fluid-mobile, thus, processes like ancient seawater alteration, prograde metamorphism (*e.g.*, release of Mg into metamorphic fluids and eclogite-host isotopic exchanges), and retrograde fluid-rock interactions (*e.g.*, interaction with metamorphic fluid during exhumation), could potentially account for the observed Mg isotopic variations. Next, we endeavor to explore how Mg isotopes behave during these processes, based on which, we highlight the importance of subduction channel fluids in generating Mg isotopic variations in exhumed eclogites.

#### *5.2.1 Seafloor alteration cannot explain the Mg isotopic signatures*

Seafloor alteration produces even larger Mg isotopic variations, with Mg isotopes likely fractionated in a different manner from that observed in the eclogites, as shown in Fig. 5. Altered oceanic crusts (AOC) from two different sites have been reported for Mg isotopic compositions (Huang et al., 2015; Teng, 2017). Carbonate-barren AOC samples recovered from IODP site 1256 in the eastern equatorial Pacific retain a mantle-like  $\delta^{26}\text{Mg}$  value as for fresh oceanic basalts (Fig. 5; Huang et al., 2015), based on which Huang et al. (2015) concluded that seafloor alteration causes limited Mg isotope fractionation, regardless of alteration temperature and water/rock ratio. At the other site (ODP site 801) in western Pacific, extensively altered AOC samples have highly variable  $\delta^{26}\text{Mg}$  values ranging from -2.76 to +0.21 (Fig. 5), with low  $\delta^{26}\text{Mg}$  values being associated with carbonate enriched samples and high  $\delta^{26}\text{Mg}$  values associated with clay-rich samples (Teng, 2017). Due to

carbonate dilution effect (Tipper et al., 2006), the AOC samples from ODP site 801 are distributed in a trend in which  $\delta^{26}\text{Mg}$  values decrease as MgO decreases (Fig. 5). Different from AOC, none of the studied eclogites (32 in total) show enrichment of light Mg isotopes, although they contain variable abundances of carbonate minerals. Furthermore, neither heavily nor less altered AOC could account for the roughly negative correlation between  $\delta^{26}\text{Mg}$  and MgO for the eclogites (Fig. 5). Thus, ancient seawater alteration is unlikely to be the cause of the variable and systemically heavier Mg isotopic compositions of the eclogites.

#### *5.2.2 The role of prograde metamorphic dehydration and eclogite-host isotopic exchange*

Magnesium isotope fractionation during prograde metamorphic dehydration or eclogite-host isotopic exchange cannot account for the Mg isotopic variations in our eclogites. It is possible that dehydrated fluids have distinct Mg isotopic compositions from the rock where the fluids are from. However, since the fraction of Mg partitioning into the fluid phases is so small compared to that inherited by metamorphic minerals during prograde metamorphism, metamorphic dehydration causes insignificant Mg isotope fractionation ( $< \pm 0.07$ ) on a bulk-rock scale (Li et al., 2011b, 2014; Teng et al., 2013; Wang et al., 2014b, 2015a, b). Local isotopic exchange between eclogite and its host rock can potentially change the original mantle-like Mg isotopic compositions of the eclogites (Wang et al., 2014a). To which direction the Mg isotopes of the eclogites fractionate depends on the types of host rock. For example, eclogite-host isotopic exchange would make eclogite boudins in carbonates/marbles isotopically lighter, whereas those enclosed in mica schists heavier (Wang et al., 2014a). However, no systemic relationship between  $\delta^{26}\text{Mg}$  and host rock type

was observed for the southwestern Tianshan eclogites. On the opposite, the carbonated eclogites (those enclosed in marbles) in our study are enriched in heavy Mg isotopes ( $\delta^{26}\text{Mg} = -0.28$  to  $+0.02$ ; Table 2), which we interpret below as a result of infiltration of external fluids derived from metasediments.

### *5.2.3 Response of Mg isotopic systematics in the eclogites to fluid-rock interactions.*

Thus, our favored interpretation of the Mg isotopic variation is fluid-rock interaction in a subduction channel. The fluids must be enriched in heavy Mg isotopes, and pervasively reactive in interacting with the eclogites because the eclogites have systemically heavier Mg isotopic compositions (Fig. 2), regardless of their diverse host rock types. Below, we discuss how the two fluid components may have affected the Mg isotopic compositions of the eclogites.

The two fluid components, due to their derivation from different hydrous minerals, have different impacts on the Mg isotopic systematics of eclogites. In the plots of  $\delta^{26}\text{Mg}$  vs.  $\text{Pb}^*$  and  $\delta^{26}\text{Mg}$  vs.  $^{87}\text{Sr}/^{86}\text{Sr}_{320\text{Ma}}$  (Fig. 6a and b), the high- $\text{Pb}^*$  and  $^{87}\text{Sr}/^{86}\text{Sr}_{320\text{Ma}}$  samples retain a mantle-like  $\delta^{26}\text{Mg}$  value, suggesting that the infiltration of high-Pb and  $^{87}\text{Sr}/^{86}\text{Sr}$  fluid component had limited influences on the Mg isotopic composition of eclogites. Being the dominant source of high-Pb and  $^{87}\text{Sr}/^{86}\text{Sr}$  component, the epidote-group minerals contain little Mg (*e.g.*, Guo et al., 2012), and thus the fluid dehydrated from them is unable to modify the Mg isotopic composition of the eclogites (although the exact  $\delta^{26}\text{Mg}$  value of any epidote-group mineral has not been reported so far). The low- $\text{Pb}^*$  and  $^{87}\text{Sr}/^{86}\text{Sr}_{320\text{Ma}}$  samples, on the other hand, have variably high  $\delta^{26}\text{Mg}$  values (Fig. 6a and b). As expected, eclogites

with high-Rb/Sr and Ba/Pb ratios have high  $\delta^{26}\text{Mg}$  values (Fig. 6c and d). Because of the complexity of the fluid system and the uncertainty of its Mg concentration and Mg isotopic composition, we are not expecting to see good correlations between  $\delta^{26}\text{Mg}$  and indices of enrichment of LILEs (such as Rb/Sr and Ba/Pb). However, the general patterns shown in Fig. 6c and d suggest that the high-LILEs component carries a significant amount of isotopically heavy Mg that has elevated the  $\delta^{26}\text{Mg}$  values of the eclogites. Mica-group minerals, as the major source of high-LILE component, are enriched in MgO, and in addition their  $\delta^{26}\text{Mg}$  values are characteristically high. For instance, biotites in metapelites from the Ivrea Zone in NW Italy have  $\delta^{26}\text{Mg}$  values ranging from -0.08 to +1.10 (Wang et al., 2015b), and phengites in eclogites from the Dabie orogen have  $\delta^{26}\text{Mg}$  values of +0.30 to +0.59 (Li et al., 2011b). Therefore, eclogites metasomatized by the mica-derived fluid could gain high- $\delta^{26}\text{Mg}$  signatures. It is also important to note that in Fig. 6c and d, a part of low-Rb/Sr and Ba/Pb samples has slightly high  $\delta^{26}\text{Mg}$  value, which we interpret as the possible influence of the talc-derived fluid, as the talc in serpentinite is depleted in LILEs but enriched in heavy Mg ( $\delta^{26}\text{Mg} = +0.06$  to  $+0.30$ ; Beinlich et al., 2014). Without good constraints on the Mg isotopic composition of fluid and the partition coefficient of MgO between fluid and eclogite, it is not yet possible to give a perfect fluid-rock interaction model for the whole dataset of the eclogites. However, the rough negative correlation between  $\delta^{26}\text{Mg}$  and MgO for the eclogites can be generally modeled as interactions of eclogites with high-MgO (*e.g.*, dehydrated from mica-group minerals or talc) and low-MgO fluid components (*e.g.*, dehydrated from epidote-group minerals) under a variety of water/rock (fluid/eclogite) ratios (Fig. 5).

### 5.3 The origins of isotopically heavy fluids in subduction channel



Fluids in subduction channels are likely to have heavy Mg isotopic compositions, although different subducted lithologies themselves show highly variable  $\delta^{26}\text{Mg}$  values. The subducted abyssal peridotites have slightly high  $\delta^{26}\text{Mg}$  values of -0.25 - +0.10 (Liu et al., 2017). The subducted sediments and altered oceanic crusts have large variations in  $\delta^{26}\text{Mg}$  values (-2.76 ‰ to +0.92 ‰), with low  $\delta^{26}\text{Mg}$  associated with carbonated rocks and with high  $\delta^{26}\text{Mg}$  associated with carbonate-free rocks (Li et al., 2010; Wang et al., 2015a; Huang et al., 2015; Teng et al., 2016; Hu et al., 2017; Teng, 2017). One might expect that subsolidus decarbonation or carbonate dissolution during metamorphism could release light Mg isotopes, making the sediment-derived fluids isotopically light. However, decarbonation is an inefficient process for carbonated sediments/basalts along the P-T paths of oceanic subduction (Gorman et al., 2006; Dasgupta and Hirschmann, 2010). Carbonate species dissolved in metamorphic fluid is thought to be mainly  $\text{CaCO}_3$  (Ague and Nicolescu, 2014; Kelemen and Manning, 2015; Li et al., 2017). Therefore, the presence of carbonate minerals in subducted rocks has negligible influence on the Mg isotopic composition of dehydrated fluids (Li et al., 2017). By contrast, breakdown of hydrous minerals might control the Mg concentration and Mg isotopic composition of dehydrated fluids. Reported  $\delta^{26}\text{Mg}$  values for Mg-rich hydrous minerals, such like mica-group minerals and talc, are higher than the normal mantle value (Li et al., 2011b; Beinlich et al., 2014; Wang et al., 2015b), and thus it is very likely that the dehydrated fluids are enriched in heavy Mg isotopes. For example, a recent study suggested that the fluid derived from talc and antigorite in serpentinite is likely characterized by high-Mg and high- $\delta^{26}\text{Mg}$ , and could be responsible for the high  $\delta^{26}\text{Mg}$  values of white schists in Western Alps (Chen et al., 2016).

## 5.4 Implications on Mg isotopic systematics in sub-arc peridotites

Fluids in subduction channels can infiltrate the mantle wedge, inducing fluid-peridotite interactions and potentially modifying the Mg isotopic composition of associated peridotites. Only a few Mg isotopic data have been reported so far for mantle wedge peridotites, and they are indeed enriched in heavy Mg isotopes: six arc peridotites from Avacha Volcano in Kamchatka analyzed by Pogge von Strandmann et al. (2011) have  $\delta^{26}\text{Mg}$  values ranging from -0.25 to -0.06, higher than the normal mantle value ( $-0.25 \pm 0.07$ ; Teng et al., 2010). Although the actual mechanism responsible for the Mg isotopic variations in these peridotites is still uncertain, their high  $\delta^{26}\text{Mg}$  values are consistent with petrological and geochemical evidence suggesting that these peridotites have been affected by upward fluid migration from the subducting slab (Ionov and Seitz, 2008). Most recently, Li et al. (2017) found that island arc or back arc basin basalts from circum-Pacific arcs, including Kamchatka, Philippines, Costa Rica and Lau Basin have generally high  $\delta^{26}\text{Mg}$  values ranging from -0.35 to +0.06. Teng et al. (2016) reported the Martinique arc lava  $\delta^{26}\text{Mg}$  values of -0.25 to -0.10. Those values overlap the Avacha peridotites and are systemically higher than normal oceanic basalts and peridotites, consistent with the interpretation that isotopically heavy fluids released from the subducted slab incorporate into the mantle wedge (Teng et al., 2016; Li et al., 2017). All the three cases suggest that massive flux of dehydrated fluid into the sub-arc mantle could facilitate extensive fluid-peridotite interaction and shift the  $\delta^{26}\text{Mg}$  of sub-arc peridotite towards higher values.

## 6. Conclusions

To reveal the nature of fluid-rock interactions in subduction channels and the influence of subduction-zone fluids on the Mg isotopic systematics in exhumed rocks, we present major and trace elements, and Sr-Nd-Mg isotopic data for the eclogites and mica schists from southwestern Tianshan, China. The following conclusions can be drawn:

- (1) The eclogites have high Ba/Rb and Ba/K but low Ce/Pb ratios, suggesting the overprint of subduction-zone metamorphic metasomatism. The highly radiogenic Sr isotopic composition ( $^{87}\text{Sr}/^{86}\text{Sr}_{320\text{Ma}} = 0.7058\text{--}0.7117$ ; higher than that of coeval seawater), together with the varying and mostly low Ni and Co concentrations, further indicate that the eclogites have interacted with fluids mainly released from subducted sediments, with limited contributions from altered oceanic crust- or serpentinite-derived fluids.
- (2) The positive correlation between  $^{87}\text{Sr}/^{86}\text{Sr}$  and  $\text{Pb}^*$ , and the bidirectional patterns in  $^{87}\text{Sr}/^{86}\text{Sr}$  - Rb/Sr,  $\text{Pb}^*$  - Rb/Sr, and  $\text{Pb}^*$  - Ba/Pb spaces, suggest interaction of the eclogites with compositionally different two fluid components: the high-LILEs component which could be derived from dehydration of mica-group minerals, and the high-Pb and  $^{87}\text{Sr}/^{86}\text{Sr}$  component likely released from epidote-group minerals in subducted sediments.
- (3) The highly variable and systemically heavy Mg isotopic compositions of eclogites ( $\delta^{26}\text{Mg} = -0.37$  to  $+0.26$  ‰) resulted from fluid-rock interactions in the subduction channel. The high-LILE component, dehydrated from Mg-rich mica-group minerals or to a less extent from talc, contains a considerable amount of Mg that has shifted the  $\delta^{26}\text{Mg}$  of the eclogites towards higher values. The high-Pb and  $^{87}\text{Sr}/^{86}\text{Sr}$

component, dehydrated from Mg-poor epidote-group minerals, has little Mg so as not to influence the Mg isotopic composition of the eclogites.

## Acknowledgement

The authors would like to thank two anonymous reviewers for insightful comments and Editor Sun-Lin Chung for careful and efficient handling. This study was financially supported by National Natural Science Foundation of China (41230209) to SGL, National Science Foundation (EAR-1340160) to FZT, and National Science Foundation of China (Grants 41330210, 41520104004) and Major State Basic Research Development Program (Grant 2015CB856105) to LFZ.

## Reference

- Agard, P., Yamato, P., Jolivet, L. and Burov, E. (2009) Exhumation of oceanic blueschists and eclogites in subduction zones: timing and mechanisms. *Earth-Science Reviews* 92, 53-79.
- Ague, J.J. and Nicolescu, S. (2014) Carbon dioxide released from subduction zones by fluid-mediated reactions. *Nature Geoscience* 7, 355-360.
- Ai, Y.L., Zhang, L.F., Li, X.P., Qu, J.F., (2006) Geochemical characteristics and tectonic implications of HP-UHP eclogites and blueschists in southwestern Tianshan, China. *Progress in Natural Science* 16, 624-632.
- Bebout, G.E. (2007) Metamorphic chemical geodynamics of subduction zones. *Earth and Planetary Science Letters* 260, 373-393.
- Bebout, G.E., Agard, P., Kobayashi, K., Moriguti, T. and Nakamura, E. (2013) Devolatilization history and trace element mobility in deeply subducted sedimentary rocks: Evidence from Western Alps HP/UHP suites. *Chemical Geology* 342, 1-20.
- Bebout, G.E., Bebout, A.E. and Graham, C.M. (2007) Cycling of B, Li, and LILE (K, Cs, Rb, Ba, Sr) into subduction zones: SIMS evidence from micas in high-P/T metasedimentary rocks. *Chemical Geology* 239, 284-304.
- Bebout, G.E. and Penniston-Dorland, S.C. (2016) Fluid and mass transfer at subduction interfaces—The field metamorphic record. *Lithos* 240–243, 228-258.

470 Beinlich, A., Klemm, R., John, T. and Gao, J. (2010) Trace-element mobilization during  
 471 Ca-metasomatism along a major fluid conduit: Eclogitization of blueschist as a consequence  
 472 of fluid–rock interaction. *Geochimica et Cosmochimica Acta* 74, 1892-1922.

473 Beinlich, A., Mavromatis, V., Austrheim, H. and Oelkers, E.H. (2014) Inter-mineral Mg  
 474 isotope fractionation during hydrothermal ultramafic rock alteration-Implications for the  
 475 global Mg-cycle. *Earth and Planetary Science Letters* 392, 166-176.

476 Busigny, V., Cartigny, P., Philippot, P., Ader, M. and Javoy, M. (2003) Massive recycling of  
 477 nitrogen and other fluid-mobile elements (K, Rb, Cs, H) in a cold slab environment: evidence  
 478 from HP to UHP oceanic metasediments of the Schistes Lustrés nappe (western Alps,  
 479 Europe). *Earth and Planetary Science Letters* 215, 27-42.

480 Carswell, D.A. (1990) Eclogite facies rocks. Blackie and Son Ltd, pp 14-49.

481 Chen, Y.-X., Schertl, H.P., Zheng, Y.-F., Huang, F., Zhou, K. and Gong, Y.-Z. (2016) Mg-O  
 482 isotopes trace the origin of Mg-rich fluids in the deeply subducted continental crust of  
 483 Western Alps. *Earth and Planetary Science Letters* 456, 157-167..

484 Chu, Z., Chen, F., Yang, Y. and Guo, J. (2009) Precise determination of Sm, Nd  
 485 concentrations and Nd isotopic compositions at the nanogram level in geological samples by  
 486 thermal ionization mass spectrometry. *Journal of Analytical Atomic Spectrometry* 24,  
 487 1534-1544.

488 Dasgupta, R. and Hirschmann, M.M. (2010) The deep carbon cycle and melting in Earth's  
 489 interior. *Earth and Planetary Science Letters* 298, 1-13.

490 Du, J.-X., Zhang, L.-F., Shen, X.-J. and Bader, T. (2014a) A new PTt path of eclogites from  
 491 Chinese southwestern Tianshan: constraints from PT pseudosections and Sm-Nd isochron  
 492 dating. *Lithos* 200, 258-272.

493 Du, J., Zhang, L., Bader, T., Chen, Z. and Lü, Z. (2014b) Metamorphic evolution of relict  
 494 lawsonite- bearing eclogites from the (U) HP metamorphic belt in the Chinese southwestern  
 495 Tianshan. *Journal of Metamorphic Geology* 32, 575-598.

496 Du, J., Zhang, L., Lü, Z. and Chu, X. (2011) Lawsonite-bearing chloritoid–glaucophane  
 497 schist from SW Tianshan, China: phase equilibria and P–T path. *Journal of Asian Earth*  
 498 *Sciences* 42, 684-693.

499 Foster G L, Pogge von Strandmann P A E. and Rae J W B. (2010) Boron and magnesium  
 500 isotopic composition of seawater. *Geochemistry, Geophysics, Geosystems* 11(8),  
 501 DOI: 10.1029/2010GC003201.

502 Gao, J., John, T., Klemm, R. and Xiong, X. (2007) Mobilization of Ti–Nb–Ta during  
 503 subduction: evidence from rutile-bearing dehydration segregations and veins hosted in  
 504 eclogite, Tianshan, NW China. *Geochimica et Cosmochimica Acta* 71, 4974-4996.

505 Gao, J. and Klemm, R. (2001) Primary fluids entrapped at blueschist to eclogite transition:  
 506 evidence from the Tianshan meta-subduction complex in northwestern China. *Contributions*  
 507 *to Mineralogy and Petrology* 142, 1-14.

508 Gao, J. and Klemm, R. (2003) Formation of HP–LT rocks and their tectonic implications in  
509 the western Tianshan Orogen, NW China: geochemical and age constraints. *Lithos* 66, 1-22.

510 Gao, J., Klemm, R., Zhang, L., Wang, Z. and Xiao, X. (1999) PT path of  
511 high-pressure/low-temperature rocks and tectonic implications in the western Tianshan  
512 Mountains, NW China. *Journal of Metamorphic Geology* 17, 621-636.

513 Gao, S., Zhang, B.-R., Gu, X.-M., Xie, Q.-L., Gao, C.-L. and Guo, X.-M. (1995)  
514 Silurian-Devonian provenance changes of South Qinling basins: implications for accretion of  
515 the Yangtze (South China) to the North China cratons. *Tectonophysics* 250, 183-197.

516 Gerya, T.V., Stöckhert, B. and Perchuk, A.L. (2002) Exhumation of high- pressure  
517 metamorphic rocks in a subduction channel: A numerical simulation. *Tectonics* 21, 6-1-6-19.

518 Glodny, J., Austrheim, H., Molina, J.F., Rusin, A.I. and Seward, D. (2003) Rb/Sr record of  
519 fluid-rock interaction in eclogites: The Marun-Keu complex, Polar Urals, Russia. *Geochimica  
520 et Cosmochimica Acta* 67, 4353-4371.

521 Gorman, P.J., Kerrick, D. and Connolly, J. (2006) Modeling open system metamorphic  
522 decarbonation of subducting slabs. *Geochemistry, Geophysics, Geosystems* 7.

523 Guo, S., Ye, K., Chen, Y., Liu, J.-B., Mao, Q. and Ma, Y.-G. (2012) Fluid-rock interaction  
524 and element mobilization in UHP metabasalt: Constraints from an omphacite-epidote vein  
525 and host eclogites in the Dabie orogen. *Lithos* 136-139, 145-167.

526 Halama, R., John, T., Herms, P., Hauff, F. and Schenk, V. (2011) A stable (Li, O) and  
527 radiogenic (Sr, Nd) isotope perspective on metasomatic processes in a subducting slab.  
528 *Chemical Geology* 281, 151-166.

529 Horodyskyj, U., Lee, C.-T.A. and Luffi, P. (2009) Geochemical evidence for exhumation of  
530 eclogite via serpentinite channels in ocean-continent subduction zones. *Geosphere* 5,  
531 426-438.

532 Hu, Y., Teng, F. -Z., Plank, T. and Huang, H.-J. (2017) Magnesium isotopic composition of  
533 subducting marine sediments. *Chemical Geology*,  
534 <http://dx.doi.org/10.1016/j.chemgeo.2017.06.010>

535 Huang, F., Chen, L., Wu, Z. and Wang, W. (2013) First-principles calculations of equilibrium  
536 Mg isotope fractionations between garnet, clinopyroxene, orthopyroxene, and olivine:  
537 Implications for Mg isotope thermometry. *Earth and Planetary Science Letters* 367, 61-70.

538 Huang, J., Ke, S., Gao, Y., Xiao, Y. and Li, S. (2015) Magnesium isotopic compositions of  
539 altered oceanic basalts and gabbros from IODP site 1256 at the East Pacific Rise. *Lithos* 231,  
540 53-61.

541 Ionov, D.A. and Seitz, H.-M. (2008) Lithium abundances and isotopic compositions in  
542 mantle xenoliths from subduction and intra-plate settings: mantle sources vs. eruption  
543 histories. *Earth and Planetary Science Letters* 266, 316-331.

544 John, T., Gussone, N., Podladchikov, Y.Y., Bebout, G.E., Dohmen, R., Halama, R., Klemm,  
545 R., Magna, T. and Seitz, H.-M. (2012) Volcanic arcs fed by rapid pulsed fluid flow through  
546 subducting slabs. *Nature Geoscience* 5, 489-492.

547 John, T., Klemm, R., Gao, J. and Garbe-Schönberg, C.-D. (2008) Trace-element mobilization  
548 in slabs due to non steady-state fluid–rock interaction: constraints from an eclogite-facies  
549 transport vein in blueschist (Tianshan, China). *Lithos* 103, 1-24.

550 John, T., Scherer, E.E., Haase, K. and Schenk, V. (2004) Trace element fractionation during  
551 fluid-induced eclogitization in a subducting slab: trace element and Lu–Hf–Sm–Nd isotope  
552 systematics. *Earth and Planetary Science Letters* 227, 441-456.

553 Kelemen, P.B. and Manning, C.E. (2015) Reevaluating carbon fluxes in subduction zones,  
554 what goes down, mostly comes up. *Proceedings of the National Academy of Sciences* 112,  
555 E3997-E4006.

556 Kelley, K.A., Plank, T., Ludden, J. and Staudigel, H. (2003) Composition of altered oceanic  
557 crust at ODP Sites 801 and 1149. *Geochemistry, Geophysics, Geosystems* 4, 890, doi:  
558 10.1029/2002GC000435.

559 Kessel, R., Schmidt, M.W., Ulmer, P. and Pettke, T. (2005) Trace element signature of  
560 subduction-zone fluids, melts and supercritical liquids at 120-180 km depth. *Nature* 437,  
561 724-727.

562 King, R.L., Bebout, G.E., Moriguti, T. and Nakamura, E. (2006) Elemental mixing  
563 systematics and Sr–Nd isotope geochemistry of mélange formation: obstacles to  
564 identification of fluid sources to arc volcanics. *Earth and Planetary Science Letters* 246,  
565 288-304.

566 Klemm, R. (2013) *Metasomatism During High-Pressure Metamorphism: Eclogites and*  
567 *Blueschist-Facies Rocks, Metasomatism and the Chemical Transformation of Rock*. Springer,  
568 pp. 351-413.

569 Klemm, R., John, T., Scherer, E., Rondenay, S. and Gao, J. (2011) Changes in dip of  
570 subducted slabs at depth: petrological and geochronological evidence from HP–UHP rocks  
571 (Tianshan, NW-China). *Earth and Planetary Science Letters* 310, 9-20.

572 Lü, Z., Zhang, L., Du, J. and Bucher, K. (2009) Petrology of coesite- bearing eclogite from  
573 Habutengsu Valley, western Tianshan, NW China and its tectonometamorphic implication.  
574 *Journal of Metamorphic Geology* 27, 773-787.

575 Lü, Z., Zhang, L., Du, J., Yang, X., Tian, Z. and Xia, B. (2012) Petrology of HP metamorphic  
576 veins in coesite-bearing eclogite from western Tianshan, China: fluid processes and  
577 elemental mobility during exhumation in a cold subduction zone. *Lithos* 136, 168-186.

578 Li, J.-L., Klemm, R., Gao, J. and John, T. (2016a) Poly-cyclic Metamorphic Evolution of  
579 Eclogite: Evidence for Multistage Burial–Exhumation Cycling in a Subduction Channel.  
580 *Journal of Petrology* 57, 119-146.

581 Li, Q.-L., Lin, W., Su, W., Li, X.-h., Shi, Y.-H., Liu, Y. and Tang, G.-Q. (2011a) SIMS U–Pb  
582 rutile age of low-temperature eclogites from southwestern Chinese Tianshan, NW China.  
583 *Lithos* 122, 76-86.

584 Li, S.-G, Yang, W., Ke, S., Meng, X.-N, Tian, H.-C., Xu, L.-J., He, Y.-S., Huang, J., Wang,  
585 X.-C., Xia, Q.-K., Sun, W.-D., Yang, X.-Y., Ren, Z.-Y., Wei, H.-Q., Liu, Y.-S., Meng, F.-C.  
586 and Yan, J. (2017) Deep carbon cycles constrained by a large-scale mantle Mg isotope  
587 anomaly in eastern China. *National Science Review* 4, 111-120.

588 Li, W.-Y., Teng, F.-Z., Ke, S., Rudnick, R.L., Gao, S., Wu, F.-Y. and Chappell, B. (2010)  
589 Heterogeneous magnesium isotopic composition of the upper continental crust. *Geochimica*  
590 *et Cosmochimica Acta* 74, 6867-6884.

591 Li, W.-Y., Teng, F.-Z., Xiao, Y. and Huang, J. (2011b) High-temperature inter-mineral  
592 magnesium isotope fractionation in eclogite from the Dabie orogen, China. *Earth and*  
593 *Planetary Science Letters* 304, 224-230.

594 Li, W.Y., Teng, F.Z., Wing, B.A. and Xiao, Y. (2014) Limited magnesium isotope  
595 fractionation during metamorphic dehydration in metapelites from the Onawa contact  
596 aureole, Maine. *Geochemistry, Geophysics, Geosystems* 15, 408-415.

597 Li, W. Y., Teng, F. Z., Xiao, Y., Gu, H. O., Zha, X. P. and Huang, J. (2016b) Empirical  
598 calibration of the clinopyroxene–garnet magnesium isotope geothermometer and  
599 implications. *Contributions to Mineralogy and Petrology* 171(7), 1-14.

600 Ling M X, Sedaghatpour F, Teng F Z., Hays, P.D., Strauss, J. and Sun, W.D. (2011)  
601 Homogeneous magnesium isotopic composition of seawater: an excellent geostandard for Mg  
602 isotope analysis. *Rapid Communications in Mass Spectrometry* 25(19): 2828-2836.

603 Liu, P.-P., Teng, F.-Z., Dick, HJB., Zhou M.-F. and Chung, S.-L (2017) Magnesium isotopic  
604 composition of the oceanic mantle and oceanic Mg cycling. *Geochimica et Cosmochimica*  
605 *Acta* 206, 151-165.

606 Miller, C., Stosch, H.-G. and Hoernes, S. (1988) Geochemistry and origin of eclogites from  
607 the type locality Koralpe and Saualpe, Eastern Alps, Austria. *Chemical Geology* 67, 103-118.

608 Plank, T. and Langmuir, C.H. (1998) The chemical composition of subducting sediment and  
609 its consequences for the crust and mantle. *Chemical geology* 145, 325-394.

610 Pogge von Strandmann, P.A.E., Elliott, T., Marschall, H.R., Coath, C., Lai, Y.-J., Jeffcoate,  
611 A.B. and Ionov, D.A. (2011) Variations of Li and Mg isotope ratios in bulk chondrites and  
612 mantle xenoliths. *Geochimica et Cosmochimica Acta* 75, 5247-5268.

613 Poli S. and Schmidt, M.W. (2002) Petrology of subducted slabs. *Annual Review of Earth and*  
614 *Planetary Sciences* 30, 207-235.

615 Pogge von Strandmann, P.A.P., Dohmen, R., Marschall, H.R., Schumacher, J.C. and Elliott,  
616 T. (2015) Extreme magnesium isotope fractionation at outcrop scale records the mechanism  
617 and rate at which reaction fronts advance. *Journal of Petrology* 56, 33-58.



618 Simons, K.K., Harlow, G.E., Brueckner, H.K., Goldstein, S.L., Sorensen, S.S., Hemming,  
619 N.G. and Langmuir, C.H. (2010) Lithium isotopes in Guatemalan and Franciscan HP–LT  
620 rocks: Insights into the role of sediment-derived fluids during subduction. *Geochimica et*  
621 *Cosmochimica Acta* 74, 3621-3641.

622 Su, W., Gao, J., Klemd, R., Li, J.-L., Zhang, X., Li, X.-H., Chen, N.-S. and Zhang, L. (2010)  
623 U–Pb zircon geochronology of Tianshan eclogites in NW China: implication for the collision  
624 between the Yili and Tarim blocks of the southwestern Altaids. *European Journal of*  
625 *Mineralogy* 22, 473-478.

626 Sun, S.-S. and McDonough, W. (1989) Chemical and isotopic systematics of oceanic basalts:  
627 implications for mantle composition and processes. Geological Society, London, Special  
628 Publications 42, 313-345.

629 Teng, F.-Z. (2017) Magnesium isotope geochemistry. *Reviews in Mineralogy &*  
630 *Geochemistry* 82, 219-287.

631 Teng, F.-Z., Hu, Y. and Chauvel, C. (2016) Magnesium isotope geochemistry in arc  
632 volcanism. *Proceedings of the National Academy of Sciences*, 201518456.

633 Teng, F.-Z., Li, W.-Y., Ke, S., Marty, B., Dauphas, N., Huang, S., Wu, F.-Y. and Pourmand,  
634 A. (2010) Magnesium isotopic composition of the Earth and chondrites. *Geochimica et*  
635 *Cosmochimica Acta* 74, 4150-4166.

636 Teng F. -Z., Li W. Y., Ke S., Yang W., Liu S. A., Sedaghatpour F., Wang S. J., Huang K. J.,  
637 Hu Y., Ling M. X., Xiao Y., Liu X. M., Li X. W., Gu H. O., Sio C., Wallace D., Su B. X.,  
638 Zhao L., Harrington M. and Brewer A. (2015) Magnesium isotopic compositions of  
639 international geological reference materials. *Geostandards and Geoanalytical Research* 39,  
640 329-339.

641 Teng, F.-Z., Wadhwa, M. and Helz, R.T. (2007) Investigation of magnesium isotope  
642 fractionation during basalt differentiation: implications for a chondritic composition of the  
643 terrestrial mantle. *Earth and Planetary Science Letters* 261, 84-92.

644 Teng, F.Z. and Yang, W. (2014) Comparison of factors affecting the accuracy of  
645 high- precision magnesium isotope analysis by multi- collector inductively coupled plasma  
646 mass spectrometry. *Rapid Communications in Mass Spectrometry* 28, 19-24.

647 Teng, F.Z., Yang, W., Rudnick, R.L. and Hu, Y. (2013) Heterogeneous magnesium isotopic  
648 composition of the lower continental crust: A xenolith perspective. *Geochemistry,*  
649 *Geophysics, Geosystems* 14, 3844-3856.

650 Tipper, E., Galy, A., Gaillardet, J., Bickle, M., Elderfield, H. and Carder, E. (2006) The  
651 magnesium isotope budget of the modern ocean: Constraints from riverine magnesium  
652 isotope ratios. *Earth and Planetary Science Letters* 250, 241-253.

653 van der Straaten, F., Halama, R., John, T., Schenk, V., Hauff, F. and Andersen, N. (2012)  
654 Tracing the effects of high-pressure metasomatic fluids and seawater alteration in  
655 blueschist-facies overprinted eclogites: Implications for subduction channel processes.  
656 *Chemical Geology* 292, 69-87.

657 van der Straaten, F., Schenk, V., John, T. and Gao, J. (2008) Blueschist-facies rehydration of  
658 eclogites (Tian Shan, NW-China): implications for fluid–rock interaction in the subduction  
659 channel. *Chemical Geology* 255, 195-219.

660 Veizer, J. (1989) Strontium isotopes in seawater through time. *Annual Review of Earth and*  
661 *Planetary Sciences* 17, 141-167.

662 Wang, S.-J., Teng, F.-Z. and Li, S.-G. (2014a) Tracing carbonate–silicate interaction during  
663 subduction using magnesium and oxygen isotopes. *Nature communications* 5.

664 Wang, S.-J., Teng, F.-Z., Li, S.-G. and Hong, J.-A. (2014b) Magnesium isotopic systematics  
665 of mafic rocks during continental subduction. *Geochimica et Cosmochimica Acta* 143, 34-48.

666 Wang, S.-J., Teng, F.-Z., Rudnick, R.L. and Li, S.-G. (2015a) The behavior of magnesium  
667 isotopes in low-grade metamorphosed mudrocks. *Geochimica et Cosmochimica Acta* 165,  
668 435-448.

669 Wang, S.-J., Teng, F.-Z. and Bea, F. (2015b) Magnesium isotopic systematics of metapelite  
670 in the deep crust and implications for granite petrogenesis. *Geochem. Perspect. Lett* 1, 75-83.

671 Wang, S.-J., Teng, F.-Z. and Scott, J. (2016) Tracing the origin of continental HIMU-like  
672 intraplate volcanism using magnesium isotope systematics. *Geochimica et Cosmochimica*  
673 *Acta* 185, 78-87.

674 Windley, B., Allen, M., Zhang, C., Zhao, Z. and Wang, G. (1990) Paleozoic accretion and  
675 Cenozoic reformation of the Chinese Tien Shan range, central Asia. *Geology* 18, 128-131.

676 Xiao, Y., Lavis, S., Niu, Y., Pearce, J.A., Li, H., Wang, H. and Davidson, J. (2012)  
677 Trace-element transport during subduction-zone ultrahigh-pressure metamorphism: Evidence  
678 from western Tianshan, China. *Geological Society of America Bulletin* 124, 1113-1129.

679 Yang, W., Teng, F.-Z. and Zhang, H.-F. (2009) Chondritic magnesium isotopic composition  
680 of the terrestrial mantle: a case study of peridotite xenoliths from the North China craton.  
681 *Earth and Planetary Science Letters* 288, 475-482.

682 Yang, X., Zhang, L.F., Tian, Z.L., Bader, T., (2013) Petrology and U-Pb zircon dating of  
683 coesite-bearing metapelites from the Kebuerte Valley, western Tianshan, China. *Journal of*  
684 *Asian Earth Sciences* 70-71, 295-307.

685 Zack, T. and John, T. (2007) An evaluation of reactive fluid flow and trace element mobility  
686 in subducting slabs. *Chemical Geology* 239, 199-216.

687 Zhang, L., Du, J., Lü, Z., Yang, X., Gou, L., Xia, B., Chen, Z., Wei, C. and Song, S. (2013) A  
688 huge oceanic-type UHP metamorphic belt in southwestern Tianshan, China: Peak  
689 metamorphic age and PT path. *Chinese Science Bulletin* 58, 4378-4383.

690 Zhang, L., Ellis, D.J. and Jiang, W. (2002) Ultrahigh-pressure metamorphism in western  
691 Tianshan, China: Part I. Evidence from inclusions of coesite pseudomorphs in garnet and  
692 from quartz exsolution lamellae in omphacite in eclogites. *American mineralogist* 87,  
693 853-860.

694 Zhang, L-F., Ellis, D., Williams, S. and Jiang, W.-B. (2003) Ultrahigh-pressure  
 695 metamorphism in eclogites from the western Tianshan, China — Reply. *American*  
 696 *Mineralogist* 88, 1157-1160.

697 Zhang, L., Lü, Z., Zhang, G. and Song, S. (2008) The geological characteristics of  
 698 oceanic-type UHP metamorphic belts and their tectonic implications: Case studies from  
 699 Southwest Tianshan and North Qaidam in NW China. *Chinese Science Bulletin* 53,  
 700 3120-3130.

701 Zhang, L., Song, S., Liou, J.G., Ai, Y. and Li, X. (2005) Relict coesite exsolution in  
 702 omphacite from Western Tianshan eclogites, China. *American Mineralogist* 90, 181-186.

703 Zhang, L., Zhang, L., Lü, Z., Bader, T. and Chen, Z. (2016) Nb–Ta mobility and  
 704 fractionation during exhumation of UHP eclogite from southwestern Tianshan, China.  
 705 *Journal of Asian Earth Sciences* 122, 136-157.

706 Zindler, A. and Hart, S. (1986) Chemical geodynamics. *Annual review of earth and planetary*  
 707 *sciences* 14, 493-571.

708

## Figure Captions

Fig. 1: Strontium and Nd isotopic compositions of the eclogites from southwestern Tianshan. MORB and OIB fields are from Zindler and Hart (1986);  $^{87}\text{Sr}/^{86}\text{Sr}$  ratio of the Ordovician to Carboniferous (O-C) seawater is from Veizer (1989), and  $^{87}\text{Sr}/^{86}\text{Sr}$  ratio of the global subducting sediments (GLOSS) can be high as much as 0.73 (Plank and Langmuir, 1998)

Fig. 2: Histogram of  $\delta^{26}\text{Mg}$  values for the eclogites from southwestern Tianshan.  $\delta^{26}\text{Mg}$  values of the eclogites with continental origin are from Li et al. (2010) and Wang et al. (2014a, b).  $\delta^{26}\text{Mg}$  values of the unaltered oceanic crust are from Teng et al. (2010).

Fig. 3: Ba/Rb vs. K (a), K/Th vs. Ba/Th (b), and Ce/Pb vs. 1/Pb (c) diagrams to differentiate between ancient seawater alteration and metamorphic metasomatism after Bebout (2007). The Ni vs. Co diagram (d) indicates that most eclogites have lower Ni and Co concentration than oceanic basalts. Data of MORB and OIB are from Sun and McDonough (1989); the Ni and Co of average serpentinite are from data compiled by van der Straaten et al. (2008).

Fig. 4: Rb/Sr vs.  $\text{Pb}^*$  (a), Ba/Pb vs.  $\text{Pb}^*$  (b),  $^{87}\text{Sr}/^{86}\text{Sr}_{(t)}$  vs.  $\text{Pb}^*$  (c) and  $^{87}\text{Sr}/^{86}\text{Sr}_{(t)}$  vs. Rb/Sr (d) diagrams to indicate the two fluid components. The  $\text{Pb}^*$  represents an indices of enrichment of Pb in the eclogites:  $\text{Pb}^* = 2 \cdot \text{Pb}_N / (\text{Ce}_N + \text{Pr}_N)$ . The higher the  $\text{Pb}^*$ , the more enrichment of Pb for the eclogites. The carbonated eclogites are marked as dashed outline. The black

triangle in panels a and b represents the average altered oceanic crust (super composite of Ocean Drilling Program Site 801) in Kelley et al. (2003). Black square and diamond represent the composition of MORB and OIB, respectively. The component 1 is enriched in LILEs, which might be derived from dehydration of mica-group minerals. The component 2 is enriched in Pb and  $^{87}\text{Sr}/^{86}\text{Sr}$ , likely released from epidote-group minerals.

Fig. 5: The variation of  $\delta^{26}\text{Mg}$  values as a function of MgO content for the eclogites (yellow circle) and mica schists (blue diamond) from southwestern Tianshan. The compositions of altered oceanic crust (AOC) from ODP site 801 and IODP site 1256 are from Huang et al. (2015) and Teng (2017). The co-variation between  $\delta^{26}\text{Mg}$  and MgO for the eclogites can be roughly modeled as fluid-rock interactions of the eclogites with compositionally different two fluid components. We assume that the component 1, because of its origin from Mg-rich mica-group minerals or to a less extent talc, have  $\delta^{26}\text{Mg} = +1.00$  and  $\text{MgO} = 1 \text{ wt.}\%$ ; the component 2, released from Mg-poor epidote-group minerals, contain very little Mg (assuming  $\text{MgO} = 0.05 \text{ wt.}\%$ ). Although we assign a value of  $+1.00$  for the  $\delta^{26}\text{Mg}$  of the low-MgO component 2, the change of this value will not affect the modelling significantly, as the component 2 contains too little Mg so as not to influence the Mg isotopic composition of the eclogites. Thus, the two purple curves with increment of 10% represent the fluid-rock interaction of an eclogite ( $\delta^{26}\text{Mg} = -0.25$ ;  $\text{MgO} = 8 \text{ wt.}\%$ ) with high-MgO and low-MgO fluid components, with the partition coefficient of MgO between fluid and eclogite,  $D_{\text{eclogite/fluid}} = 4$ . The black dotted curve represents binary mixing between sediments and basalts, which suggests that  $>60\%$  of sedimentary component is required to produce the Mg

isotopic composition of the eclogites. The green bar represents the normal mantle  $\delta^{26}\text{Mg}$  value (Teng et al., 2010).

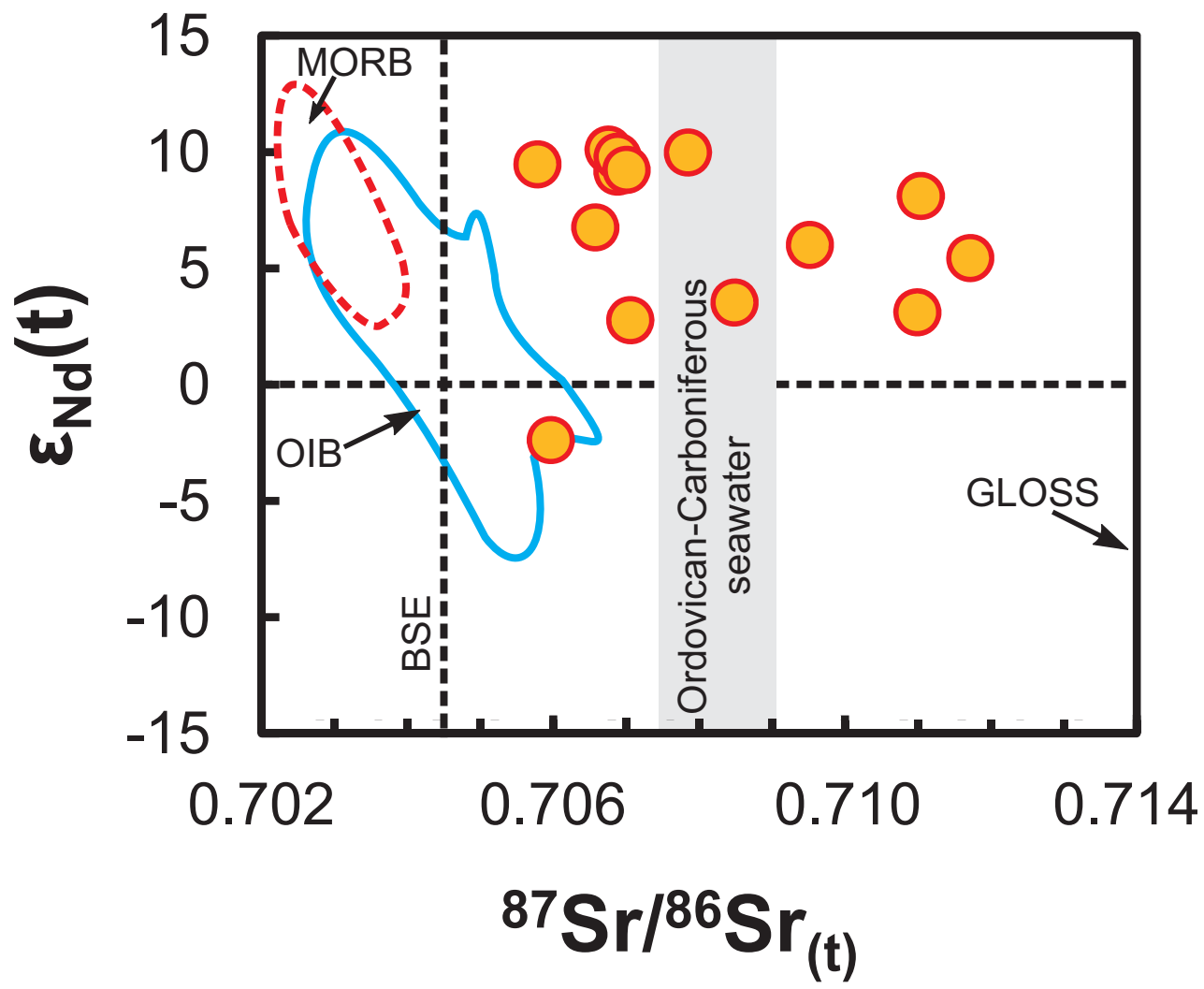
Fig. 6:  $\delta^{26}\text{Mg}$  vs.  $\text{Pb}^*$  (a),  $\delta^{26}\text{Mg}$  vs.  $^{87}\text{Sr}/^{86}\text{Sr}_{(t)}$  (b),  $\delta^{26}\text{Mg}$  vs.  $\text{Rb}/\text{Sr}$  (c), and  $\delta^{26}\text{Mg}$  vs.  $\text{Ba}/\text{Pb}$  (d) diagrams showing the influence of the two fluid components on the Mg isotopic systematics of eclogites (shown as solid arrows). The carbonated eclogites are marked as dashed outline. The high-LILE fluid component contains a considerable amount of isotopically heavy Mg to shift the  $\delta^{26}\text{Mg}$  of eclogites towards a higher value, whereas the high- $^{87}\text{Sr}/^{86}\text{Sr}$  and -Pb fluid component contains little heavy Mg to influence the Mg isotopic systematics of eclogites. Some low-Rb/Sr and -Ba/Pb samples also have slightly heavy Mg isotopic compositions, which might point towards the contributions of fluids dehydrated from talc in serpentinite (shown as dashed arrows; Beinlich et al., 2014).

## Table Captions

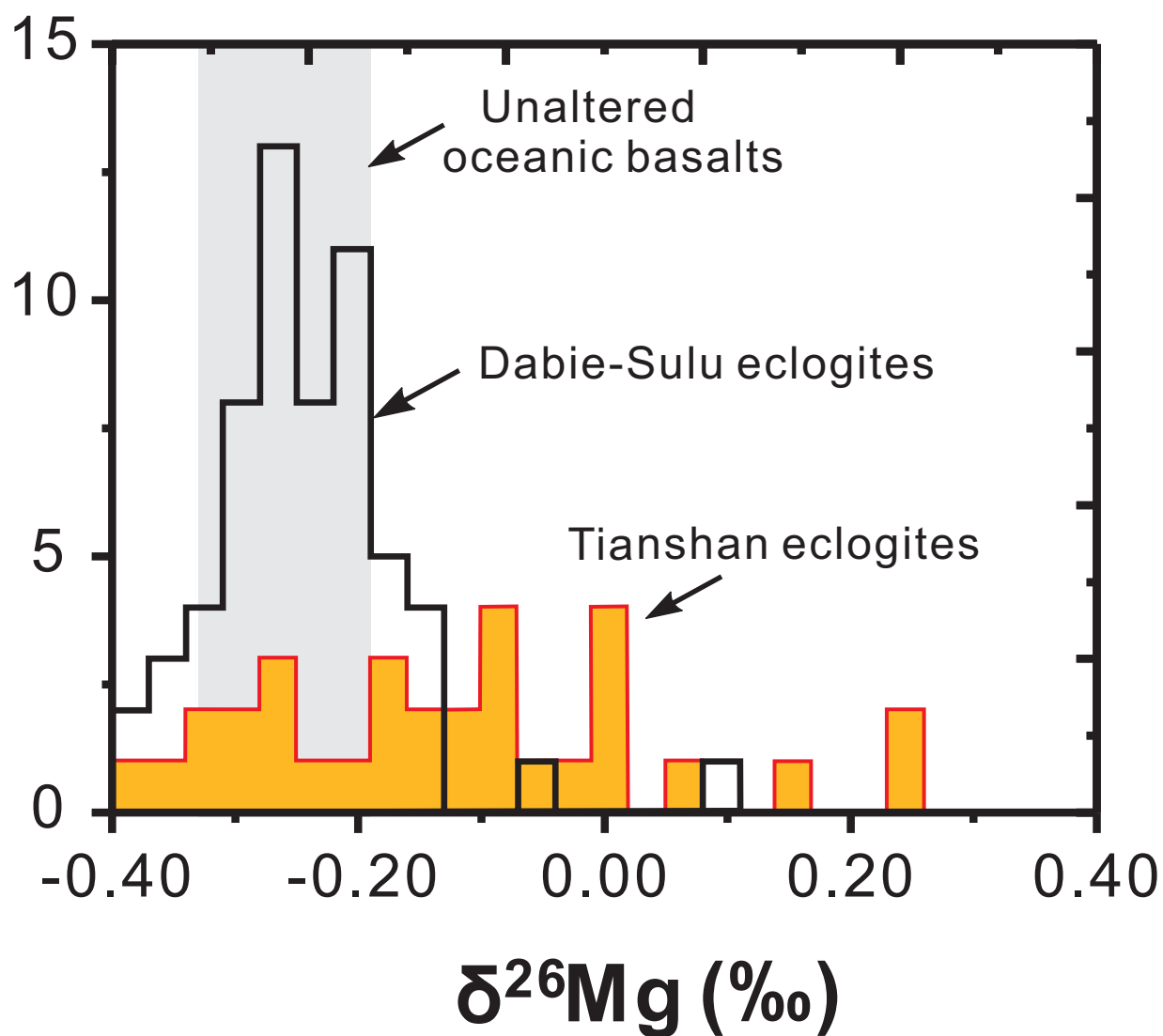
Table 1. Strontium and Nd isotopic compositions of the eclogites from southwestern Tianshan.

Table 2. Magnesium isotopic compositions of the eclogites and mica schists and their mineral separates from southwestern Tianshan.

*Figure. 1 Wang et al.*



*Figure. 2 Wang et al.*





*Figure. 3 Wang et al.*

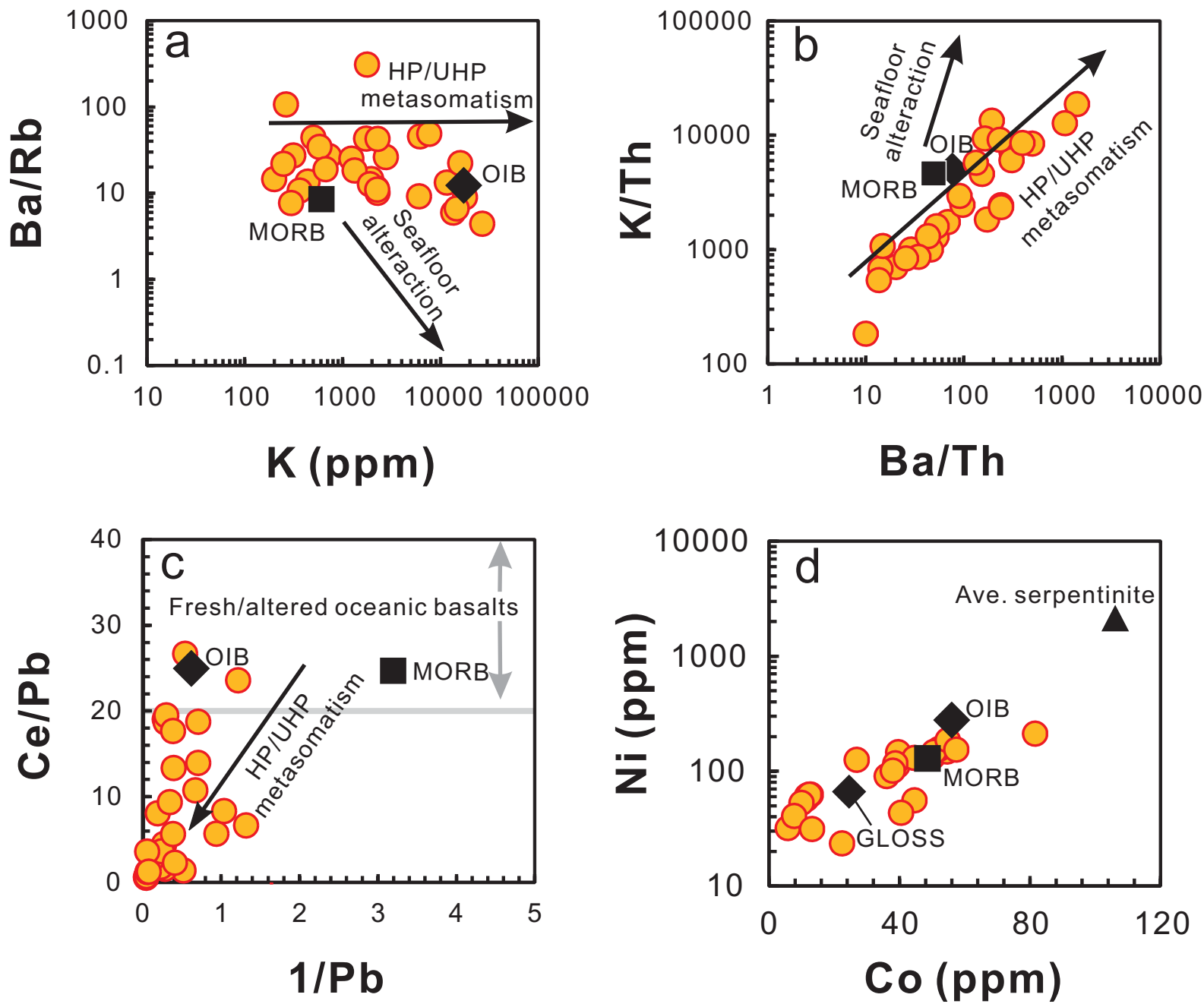


*Figure. 4 Wang et al.*

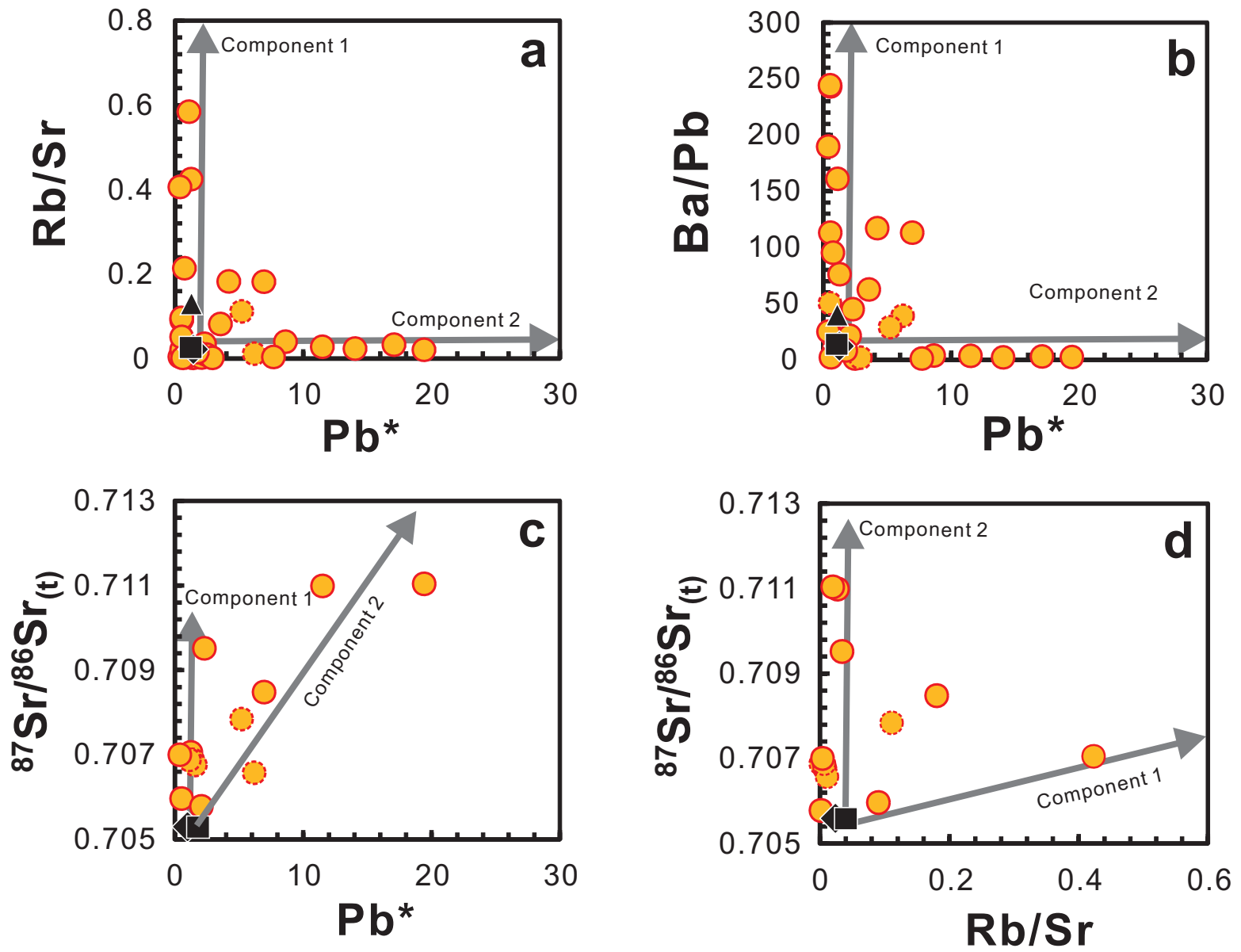


*Figure. 5 Wang et al.*

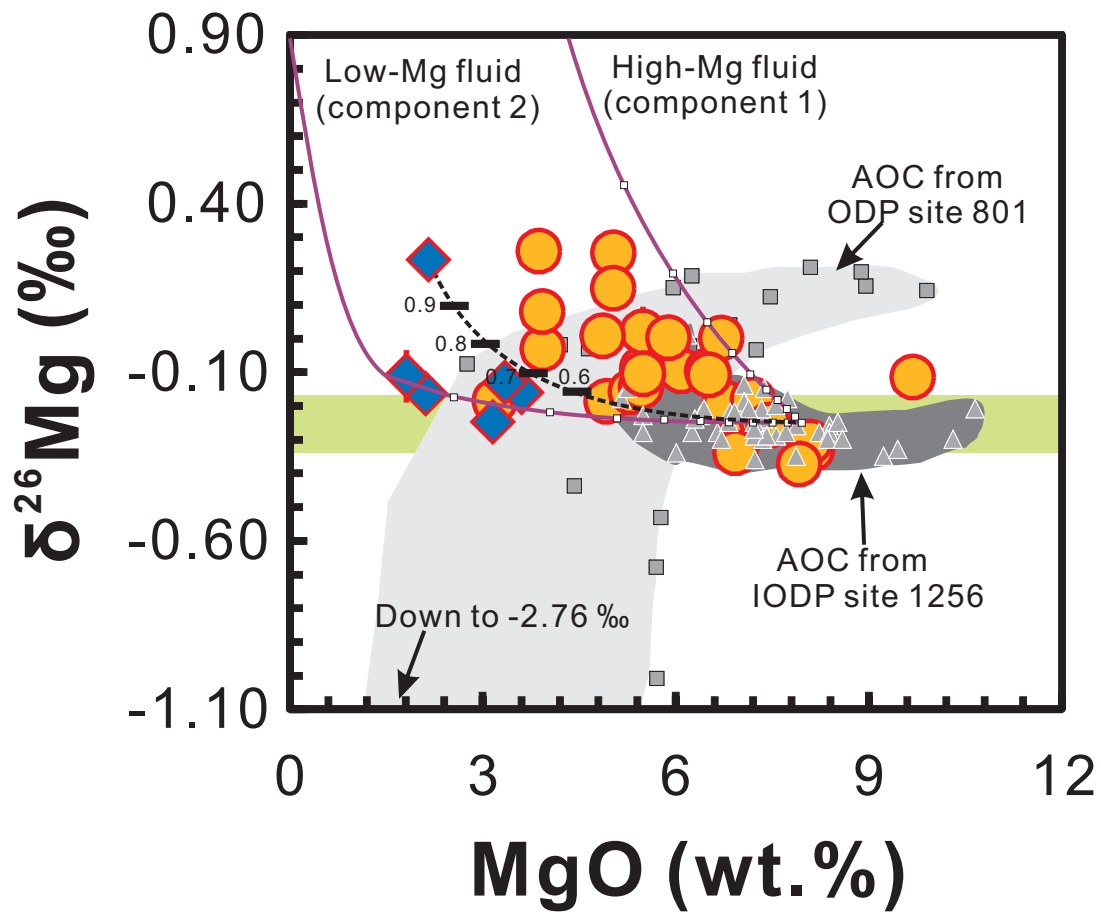
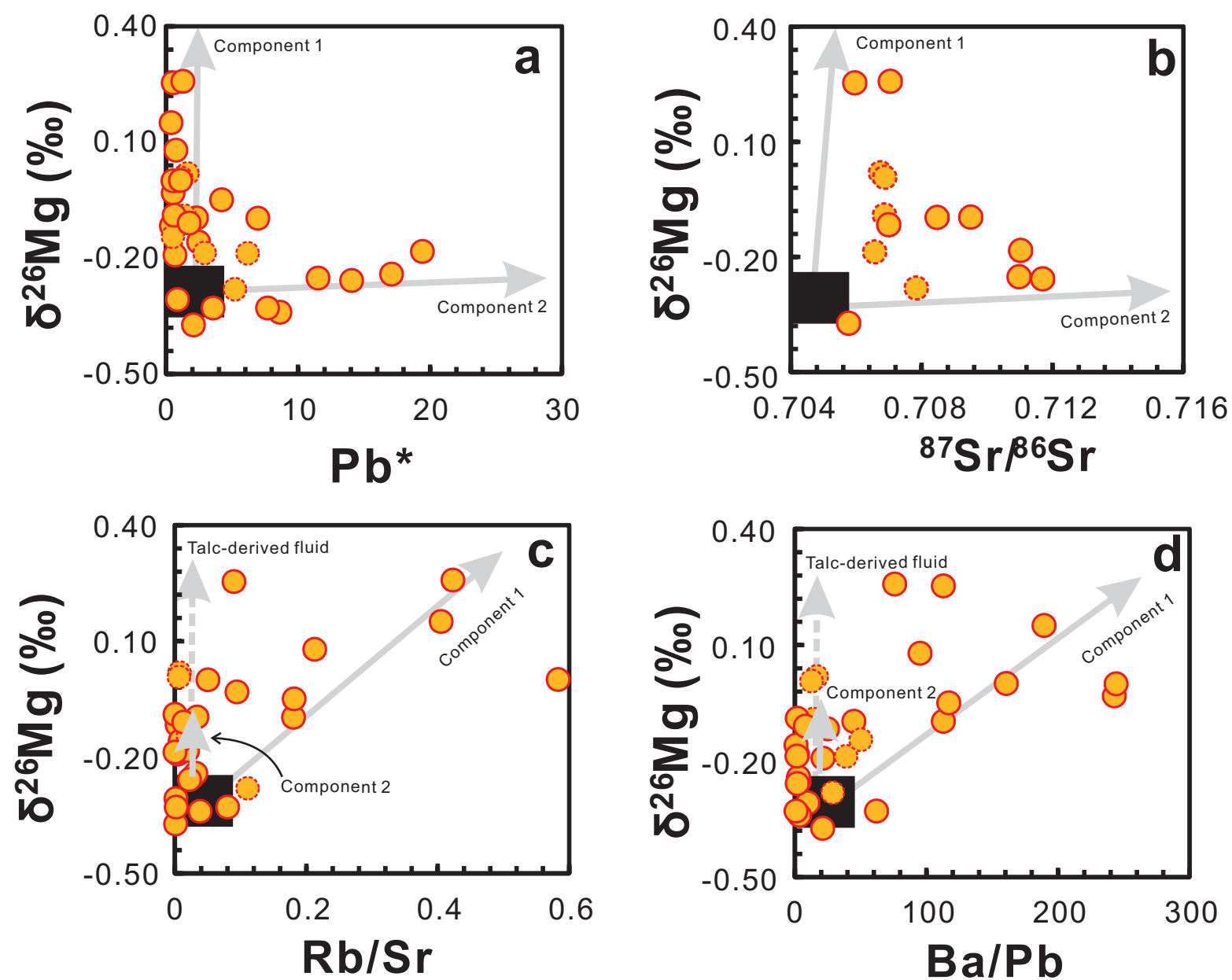


*Figure. 6 Wang et al.*



1 Table 1. Strontium and Nd isotopic compositions of the eclogites from southwestern Tianshan

2

Sample	Rb(ppm)	Sr(ppm)	<sup>87</sup> Rb/ <sup>86</sup> Sr	<sup>87</sup> Sr/ <sup>86</sup> Sr	2sigma	<sup>87</sup> Sr/ <sup>86</sup> Sr <sub>(320Ma)</sub>	Sm(ppm)	Nd(ppm)	<sup>147</sup> Sm/ <sup>144</sup> Nd	<sup>143</sup> Nd/ <sup>144</sup> Nd	2sigma	εNd <sub>(320Ma)</sub>
H902-7	31.1	332	0.271	0.707198	0.000006	0.7060	9.35	37.6	0.150	0.512418	0.000007	-2.4
300-1	89.2	203	1.275	0.712858	0.000045	0.7071	5.74	23.1	0.150	0.512682	0.000011	2.8
H902-4	3.9	115	0.099	0.709964	0.000004	0.7095	3.35	11.5	0.176	0.512903	0.000016	6.0
H902-5	8.5	47.0	0.523	0.710863	0.000004	0.7085	0.67	1.94	0.207	0.512841	0.000026	3.5
305-1 <sup>a</sup>	0.8	92.3	0.024	0.706988	0.000006	0.7069	1.51	4.47	0.204	0.513122	0.000012	9.2
305-2 <sup>a</sup>	1.4	181	0.022	0.706855	0.000006	0.7068	2.01	5.46	0.222	0.513209	0.000016	10.1
305-3 <sup>a</sup>	9.1	273	0.097	0.707012	0.000007	0.7066	1.32	4.23	0.188	0.512966	0.000024	6.8
305-4 <sup>a</sup>	5.0	42.8	0.338	0.709384	0.000008	0.7078	2.4	6.56	0.221	0.513201	0.000016	10.0
X3-1 <sup>a</sup>	1.1	175	0.018	0.706961	0.000008	0.7069	2.43	6.92	0.212	0.513172	0.000007	9.8
8-12	4.0	297	0.039	0.711889	0.000008	0.7117	3.09	9.50	0.196	0.512917	0.000009	5.4
H608-6	5.4	149	0.105	0.711467	0.000003	0.7110	3.14	10.2	0.186	0.512775	0.000019	3.1
8-4	2.6	128	0.058	0.711301	0.000007	0.7110	2.34	7.37	0.191	0.513043	0.000034	8.1
8-9	0.4	112	0.011	0.707053	0.000004	0.7070	3.92	13.2	0.179	0.513076	0.000013	9.2
8-20	4.4	170	0.075	0.706122	0.000007	0.7058	5.11	16.3	0.189	0.513108	0.000017	9.5

3 Note: Samples marked with a superscript “a” are carbonated eclogites enclosed in marbles, and all the others are the eclogites enclosed in mica schists

4

5 Table 2. Magnesium isotopic compositions of the eclogites and mica schists and their mineral  
6 separates from southwestern Tianshan.

Sample	Rock/Mineral	$\delta^{26}\text{Mg}$	2SD	$\delta^{25}\text{Mg}$	2SD
<i>Eclogites/blueschists</i>					
H902-7	Bulk rock	0.27	0.08	0.16	0.05
	Replicate	0.24	0.06	0.14	0.08
	average	0.25	0.05	0.15	0.04
	Grt	-1.37	0.07	-0.69	0.06
	Cpx	0.46	0.07	0.27	0.06
300-1	Bulk rock	0.25	0.05	0.16	0.04
	Replicate	0.28	0.07	0.15	0.05
	average	0.26	0.04	0.16	0.04
H902-4	Bulk rock	-0.10	0.05	-0.03	0.04
	Grt	-1.61	0.07	-0.88	0.06
	Duplicate	-1.70	0.07	-0.87	0.05
	average	-1.66	0.05	-0.87	0.04
	Cpx	0.09	0.05	0.02	0.07
	Replicate	0.05	0.05	0.04	0.07
	average	0.07	0.04	0.03	0.05
H902-5	Bulk rock	-0.10	0.06	-0.04	0.05
	Grt	-1.58	0.07	-0.78	0.07
	Duplicate	-1.47	0.09	-0.77	0.06
	average	-1.54	0.06	-0.78	0.04
	Cpx	0.06	0.05	0.01	0.07
H907-21	Bulk rock	-0.19	0.06	-0.11	0.05
	<b>Grt</b>	-1.45	0.09	-0.76	0.06
	Cpx	-0.04	0.05	-0.05	0.07
305-1 <sup>a</sup>	Bulk rock	-0.09	0.05	-0.07	0.05
	Grt	-1.10	0.07	-0.58	0.05
	Cpx	0.14	0.07	0.09	0.05
305-2 <sup>a</sup>	Bulk rock	0.02	0.08	0.02	0.05
	Grt	-1.17	0.06	-0.60	0.05
	Duplicate	-1.16	0.06	-0.64	0.05
	Replicate	-1.16	0.09	-0.59	0.06
	average	-1.16	0.04	-0.62	0.03
	Cpx	0.11	0.07	0.04	0.05
305-3 <sup>a</sup>	Bulk rock	-0.19	0.06	-0.10	0.03
305-4 <sup>a</sup>	Bulk rock	-0.28	0.05	-0.16	0.04
X3-1 <sup>a</sup>	Bulk rock	0.01	0.06	-0.01	0.05
	Grt	-1.16	0.06	-0.63	0.04
	Duplicate	-1.15	0.09	-0.60	0.06
	average	-1.16	0.05	-0.62	0.03
8-12	Bulk rock	-0.26	0.05	-0.13	0.04

8-19	Bulk rock	-0.33	0.05	-0.19	0.05
	Grt	-1.54	0.07	-0.79	0.06
	Replicate	-1.52	0.06	-0.75	0.06
	Duplicate	-1.51	0.07	-0.80	0.06
	average	-1.52	0.04	-0.78	0.03
	Cpx	0.27	0.07	0.13	0.05
8-26	Bulk rock	-0.31	0.05	-0.16	0.05
H608-6	Bulk rock	-0.25	0.05	-0.11	0.04
	Grt	-1.56	0.07	-0.81	0.05
8-3	Bulk rock	-0.24	0.05	-0.13	0.04
	Grt	-1.51	0.09	-0.83	0.06
8-4	Bulk rock	-0.17	0.05	-0.10	0.05
	Replicate	-0.19	0.06	-0.09	0.05
	average	-0.18	0.04	-0.10	0.04
	Grt	-1.67	0.07	-0.87	0.07
	Duplicate	-1.65	0.09	-0.87	0.06
	average	-1.66	0.06	-0.87	0.04
8-5	Bulk rock	-0.26	0.05	-0.13	0.04
	Grt	-1.34	0.07	-0.70	0.06
8-7	Bulk rock	-0.34	0.06	-0.15	0.05
8-9	Bulk rock	-0.12	0.06	-0.05	0.05
8-20	Bulk rock	-0.37	0.05	-0.16	0.05
	Grt	-1.75	0.07	-0.89	0.05
	Cpx	-0.02	0.07	-0.03	0.05
H710-3	Bulk rock	-0.16	0.05	-0.03	0.05
A314-3 <sup>a</sup>	Bulk rock	-0.15	0.08	-0.08	0.05
	Grt	-1.53	0.07	-0.80	0.05
	Cpx	0.45	0.05	0.26	0.07
105-1	Bulk rock	-0.03	0.07	-0.03	0.06
105-12	Bulk rock	0.00	0.07	0.02	0.06
106-14 <sup>a</sup>	Bulk rock	-0.19	0.07	-0.12	0.06
110-3	Bulk rock	0.08	0.07	0.01	0.06
Q316-10	Bulk rock	-0.09	0.04	-0.04	0.02
A300-3	Bulk rock	0.00	0.03	0.00	0.03
a300-16	Bulk rock	-0.11	0.04	-0.05	0.02
H902-10	Bulk rock	-0.33	0.02	-0.16	0.02
k984 - 1	Bulk rock	-0.05	0.06	-0.02	0.03
H902-2 - 1	Bulk rock	0.15	0.01	0.07	0.01
<u>Mica schist</u>					
106-3B	Bulk rock	-0.18	0.07	-0.08	0.06
	Duplicate	-0.13	0.08	-0.05	0.05
	average	-0.16	0.05	-0.06	0.04
986-1	Bulk rock	-0.11	0.08	-0.02	0.05
305-5	Bulk rock	-0.16	0.05	-0.08	0.04

Q314-1	Bulk rock	0.23	0.02	0.13	0.03
Q316-4	Bulk rock	-0.25	0.02	-0.13	0.01
H865 - 1	Bulk rock	-0.13	0.03	-0.06	0.01

---

- 7 Note:
- 8 Samples marked with a superscript “a” are carbonated eclogites enclosed in marbles, and all the
- 9 others are the eclogites enclosed in mica schists; Grt = garnet; Cpx = clinopyroxene;
- 10 2SD = two times the standard deviation of the population of n (n>20) repeat measurements of the
- 11 standard during an analytical session;
- 12 Replicate: repeat sample dissolution, column chemistry and instrument analysis of Mg isotopic ratios;
- 13 Duplicate: repeat measurement of Mg isotopic ratios on the same solution.



**LaTeX Source Files**

[Click here to download LaTeX Source Files: 2017 June 20\\_Supplement.docx](#)